




Montanuniversität Leoben

Master's Thesis



Drill Stem Failure Analysis During
Fishbone Wells Construction in the East
Messoyakha Field

Artur Khusnutdinov

May 2019

Dedicated to my parents, Amina and Renis.

Affidavit

I declare in lieu of oath that I wrote this thesis and performed the associated research myself using only literature cited in this volume.



Artur Khusnutdinov, 28 May 2019

Abstract

Horizontal drilling for production wells has almost completely displaced the vertical and conventional directional drilling, which led to the significant revision of drill string technical requirements. The need for constant monitoring of the technical condition of various drill stem elements is becoming a mandatory process.

Moreover, one of the most widespread accident in drilling is a drill stem failure including pipe washouts and drill string breakdowns.

The issue of early prevention of drill stem accidents has always been a critical question since the rotary drilling appearance. For example, an accident analysis on the areas of the Timan-Pechora province indicated that 42% of all accidents from 1971 to 2013 are accidents with drill stem elements. This is a statistics without taking into account sticking (Kamenskikh 2015). However, even since 2013, the speed and footage of drilling has increased significantly. Drill string failures due to fatigue wear of the pipe body and tool joints has become a common problem in drilling companies. In addition to the non-productive time spent on the elimination of such accidents, companies suffer huge losses associated with the disposal of nonserviceable pipes and expensive bottom hole assemblies (BHA) left in the well.

The thesis focuses on a problem of drill stem failures during drilling of high-tech wells in the East Messoyakha oil field. Key features, conditions and causes of accidents are discussed. The ways to eliminate the same problems in the further work are considered and estimated from economic and technical point of view.

Zusammenfassung

Horizontales Bohren für Produktionsbohrung hat fast gänzlich vertikales und konventionelles gerichtetes Bohren ersetzt. Das hat zum wesentlichen Durchbruch von Bohrgestängestrang der technischen Anforderungen geführt. Das Bedürfnis ständiger Überwachung von technischen Beschaffenheiten von verschiedenen Bohrstangelementen wird ein befehlender Prozess.

Außerdem, die weitverbreiteste Störung in Bohren ist Bohrstangestörung, einschließlich Rohrauswaschung und Bohrgestängestrangauffälle.

Das Problem von früherer Vorbeugung von Bohrstangenausfällen ist ein akutes Problem seit Drehbohren geworden. Zum Beispiel, die Ausfallanalyse an Timan-Pechora Gegend hat gezeigt an, dass 42% von allen Ausfällen seit 1971 bis 2013 mit Bohrstangelementen verbunden ist. Diese Statistik schließt nicht Bohrstangenspannprätze um (Kamenskikh 2015). Jedoch, seit 2013 haben sich Tempo und Umfang von Bohren wesentlich vergrößert. Bohrstangenausfälle werden wegen des Ermüdungsverschleiß von Rohrkörper und Rohrverbindungen zum allgemeinen Problem für die Bohrunternehmer. Zuzüglich zur unproduktiven Beseitigungszeit dieser Ausfälle erledigen Gesellschaften großen Verlust, der mit der Entsorgung von unbetriebsfähigen Rohren und eine teure Rohrschuhauflösung verbunden ist.

Die Dissertation ist dem Problem von der Bohrstangestörung während des Bohrens von high-tech Bohrlöchern in Osten Messoyakha Ölfield. Haupteigenschaften, Bedingungen und Ursachen von Ausfällen sind besprochen. Die Hauptwege der Verhinderung solcher Probleme in künftigen Bohrlöchern waren besprochen vom wirtschaftlichen und technologischen Gesichtspunkt aus.

Acknowledgements

I would first like to thank my university thesis advisors Univ.-Prof. Mikhail Gelfgat and Univ.-Assoc. Prof. Alexey Arkhipov for helping and keeping me on the right way in my research. In addition, Mikhail Gelfgat, Univ.-Assoc. Prof. Vladimir Balitsky and Univ.-Assoc. Prof. Michael Prohaska were the ones who dealt with most of the difficulties in our educational process, what I am thankful for too.

I would like to thank Gazpromneft STC personnel including:

Head of Drilling & Downhole Treatment Department Konstantin Kulakov for assignment the opportunity to have internship in the company;

Drilling & Downhole Treatment Department Specialist Artem Zakirov for supervising me during the whole period of thesis writing;

Drilling & Downhole Treatment Department Specialist Anton Sokolov for helping me in questions of accidents analysis and providing me all necessary data;

Project Manager Konstantin Pryadilov for initiation my internship in the company;

Head of Human Resources Department Pavel Sorokin for consulting me in terms of the internship and contracts.

I would like to thank other people who in any way supported me during this period: Galiya Khayrullina, Alexander Verkhozin, Fanil Gatiatullin, Artem Karimov, Yaroslav Kuprin, Pouya Ziashahabi, Renat Dzhafarov, Daria Amitirova-Turgeneva, Timur Mufazalov, Yasin Naseri and many others including both university staff, my family and friends.

Thanks to all of you, I've got the power.

Contents

| | |
|---|----|
| Chapter 1 Introduction..... | 1 |
| 1.1 Project Objectives..... | 1 |
| 1.2 Project Inputs..... | 2 |
| Chapter 2 Drill Stem Regulations | 3 |
| 2.1 Background..... | 3 |
| 2.2 International Standards for Drill Stem Elements | 4 |
| 2.2.1 API Standards | 5 |
| 2.2.2 DS-1 Standards..... | 7 |
| 2.2.3 NS-2 Standard | 9 |
| 2.3 Russian Standards for Drill Stem Elements | 9 |
| 2.3.1 State Standards of Russian Federation | 9 |
| 2.3.2 Guidance Document of PJSC Gazprom Neft..... | 10 |
| 2.4 Chapter Summary..... | 12 |
| Chapter 3 Field Data Analysis..... | 13 |
| 3.1 General Overview..... | 13 |
| 3.2 Lithostratigraphic Characteristics of the Deposit..... | 14 |
| 3.3 Possible Complications in Wells..... | 15 |
| 3.4 Well Profile | 16 |
| 3.5 Used Drill String Components and Drilling Parameters | 18 |
| 3.6 Problem Description in the East Messoyakha Field | 19 |
| 3.7 Chapter Summary..... | 24 |
| Chapter 4 Actual Loads Analysis Received by Drill Stem Elements During Well #1 Construction..... | 25 |
| 4.1 Accident Description..... | 26 |
| 4.2 Tensile Load Analysis | 28 |
| 4.3 Torque Analysis | 32 |
| 4.4 Buckling Analysis | 34 |
| 4.5 Tri-axial Loading Analysis | 42 |
| 4.6 Chapter Summary..... | 45 |
| Chapter 5 Drill Pipe Technical Expertise Conclusions | 47 |
| 5.1 Subject of research and documentation review | 47 |
| 5.2 The purpose and order of the study..... | 48 |

| | |
|--|----|
| 5.3 Verification of the chemical composition, phase structure and mechanical properties of the metal | 48 |
| 5.4 Fractography Studies..... | 50 |
| 5.5 Number of Cycles to Failure Analysis (on samples with and without a stress concentrator)..... | 53 |
| 5.6 Structure and hardness analysis | 56 |
| 5.7 Mudlogging Data Analysis Based on the Technical Expertise | 57 |
| 5.8 Chapter Summary..... | 59 |
| Chapter 6 Fatigue Analysis..... | 61 |
| 6.1 Theory of Fatigue | 61 |
| 6.2 Implementation of TH Hill Curvature Index Approach | 63 |
| 6.2.1 Curvature Index curves | 63 |
| 6.2.2 Comparative design approach..... | 64 |
| 6.3 Lubinski Curves | 67 |
| 6.4 Chapter Summary..... | 69 |
| Chapter 7 Recommendations..... | 71 |
| 7.1 Buckling effect elimination | 71 |
| 7.2 Dogleg severity control | 73 |
| 7.3 Drill Pipes Washouts Detection | 74 |
| 7.4 Drill Pipes Operating Time Recording..... | 74 |
| 7.5 Chapter Summary..... | 77 |
| Chapter 8 Conclusions..... | 78 |

Chapter 1 Introduction

Horizontal drilling for production wells has almost completely displaced the vertical and conventional directional drilling, which led to the significant revision of drill string technical requirements. The need for constant monitoring of the technical condition of various drill stem elements is becoming a mandatory process.

Moreover, one of the most widespread accident in drilling is a drill stem failure including pipe washouts and drill string breakdowns.

The issue of early prevention of drill stem accidents has always been a critical question since the rotary drilling appearance. For example, an accident analysis on the areas of the Timan-Pechora province indicated that 42% of all accidents from 1971 to 2013 are accidents with drill stem elements. This is a statistics without taking into account sticking (Kamenskikh 2015). However, even since 2013, the speed and footage of drilling has increased significantly. Drill string failures due to fatigue wear of the pipe body and tool joints has become a common problem in drilling companies. In addition to the non-productive time spent on the elimination of such accidents, companies suffer huge losses associated with the disposal of nonserviceable pipes and expensive bottom hole assemblies (BHA) left in the well.

PJSC Gazprom Neft has been improving high-tech approaches in well drilling year to year out. One of the most complex and technically equipped drilling projects is the East Messoyakha field development, where the mode of the hydrocarbon occurrence dictate terms for the pay zones management. The fishbone multilateral wells has been started to implement since 2016. Moreover, rotary steerable system (RSS) technology us is being used for the best borehole quality and high rates of penetration.

The combination of complex trajectories, high dogleg severity values, drilling parameters with high revolution and pressure rates have a tremendous impact on the drill stem elements. Since 2017, three drill string failures and dozens of pipe washouts were recorded at the facilities of JSC Messoyakhaneftegaz. It indicates the need to review these incidents in order to identify possible causes of their occurrence and draw up recommendations on how to prevent drill stem breakdowns in the future.

1.1 Project Objectives

The thesis purpose is to analyze failures from different perspectives trying to find the main reasons for those situations and the means of further problems elimination.

Objectives to reach the purpose:

- Compare various approaches of drill stem standardization taking into account both – International and Russian standards;
- Investigate field data to get acquainted with general pattern of problem;
- Do laboratory study on broken part of pipe and make conclusions;

Introduction

- Computation of loads to define were there any overloading conditions (axial, tri-axial, torque and drag analysis);
- Analyze fatigue life of tubulars using comparative-design approach by T. H. Hill;
- Draw an inference about possible ways to eliminate the same problems related to drill stem failures in the future.

1.2 Project Inputs

The most of data for accident analysis was received from Gazpromneft Science & Technology Centre. This includes broad range of documents, equipment certificates, field data, reports, accident descriptions etc.

One of the key instruments for problem evaluation was an access to mudlogging data, which can throw light on many aspects of drilling process.

Prior to analyze itself the actual well profiles and BHA were designed in Landmark software (Compass, WellPlan packages). Seven fishbone laterals and main borehole of the emergency well were constructed including real trajectory, drilling mud data, friction coefficients etc.

Moreover, a contract for broken drill pipe metal technical expertise was signed between drilling contractor and Gubkin University laboratory. The results of that expertise helped a lot in understanding of accident progression.

Chapter 2 Drill Stem Regulations

2.1 Background

The oil and gas industry is one of the largest consumer of various types of pipes. They are divided into three large groups: drilling, casing and tubing.

With the rotary drilling appearance at the turn of the XIX – XX centuries, petroleum engineers started to think about improving the drill pipes. The first pipes with fine threads turned out to be inapplicable for a number of reasons:

- the slightest inaccuracies in the derrick align led to the thread jamming due to skewing;
- makeup operation was time-consuming;
- thread wore out quickly, no way to withstand multiple make-ups;
- thread was acting as a stress concentrator.

In addition, pipes were made from low carbon steel, and their strength was insufficient.

In 1910, the American engineer Witter made a real breakthrough, inventing tool joints with a conical buttress thread with the coarse pitch, which were connected to the pipe body by means of a fine pitch conical thread of a triangular profile.

In 1914, pipes of more durable steel appeared, and in 1919 – pipes with internal upset, which compensated for the decrease in wall thickness occurred during thread cutting. This design became the basis for the creation of GOST 631 in Soviet Union, the latest edition of which was approved in 1975.

Further searches for various hardening methods led to the development of bulk heat treatment in 1919, and this helped to increase the life of the tool joint thread.

At the same time, attempts were made to replace pipe threads by creating samples with a monolithic construction tool joint and pipe body. The first such example with thick-walled upsets at both ends of the pipe was created in 1931. Directly at the upset, a thread was cut, however, this type of pipe was not widely used for several reasons:

- the need to manufacture the entire pipe from expensive alloy steel;
- due to the considerable dimensions of the product, the possibility of various methods of the thread hardening is complicated or eliminated;
- the unfavorable macrostructure reduces thread fatigue limit;
- more complicated metrological control of the thread.

However, the main cause of accidents in toll-jointed pipes was the same fatigue damage along fine pitch thread. It was possible to get rid of these problems by creating pipes with conical shouldered connection (Figure 1).

Drill Stem Regulations

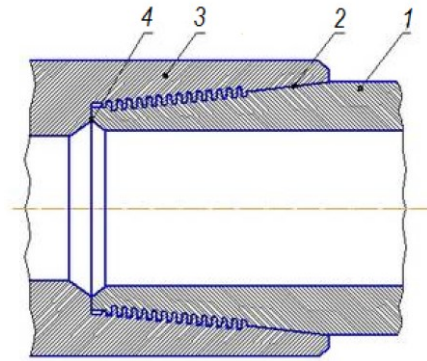


Figure 1: Example of tool joint with conical shouldered connection.

1 – pipe body, 2 – conical stabilizing shoulder, 3 – tool joint box, 4 – inside thrust face

The next stage in the development of the pipe design was the creation of a solid joint by welding the connection with the pipe. These works were begun in 1937.

In the 50s, the first domestic welded pipes appeared. They had a marked seam, which was a stress concentrator. Weld was performed on the body of the pipe without any upset. This design was fragile, but justified by the lack of additional friction losses, which was important for turbine drilling. Later, for hardening of the structure, the upset appeared in these pipes. After all, the previous upset was created to increase the strength under the thread, here to increase the weld itself.

Later, the weld was transferred to the internal upset of pipes manufactured according to TU 14-3-577-77. However, they also had low fatigue strength, consequently, coming out of use in the industry.

After many experiments, the USSR Ministry of Oil Industry acquired in Germany ready-made lines for the manufacture of drill pipes, where locks were welded with friction and non-destructive testing operations were included in the process. Currently, these pipes are produced according to GOST R 50278-92. Their quality is comparable with foreign analogues (Aizupe and Polyachek 2012).

2.2 International Standards for Drill Stem Elements

At the moment, in international practice, several organizations have gained wide industrial distribution in the field of drill pipes and bottom-hole assemblies (BHA) standardization.

The API (American Petroleum Institute) is the first global community to begin regulating issues in the oil and gas industry. The first standards were published by this organization in 1924. Today, the institute covers about 500 standards in all segments of the oil and gas industry (<https://www.api.org/> 2019).

Bureau Veritas is one of the largest inspection and certification companies in the world, based in France. It was originally created as a bureau for the inspection, supervision and verification of ships and cargo. Now, on the basis of this company, T. H. Hill Associates Inc., an organization engaged in the standardization of downhole

equipment, carries out its activities. The founder and ideologist of the organization is an American engineer Thomas Hill (T. H. Hill Associates, Inc 2012).

O.C.T.G. Procter Consultancy Limited is a drilling tools control and standardization company previously owned under various Exxon trademarks. It gained independence in order to further develop and distribute its proposals outside of Exxon. Published the first version of the standard NS-2 in 1999 (Fearnley 2003).

2.2.1 API Standards

API standards include three main documents:

- Technical requirements for drill pipe – 5DP;
- Technical requirements for drill stem elements in rotary drilling – Spec 7-1;
- Technical requirements for threaded connections and Measurement of drill pipe joints – Spec 7-2.

The international standard 5DP defines technical conditions for the steel drill pipes with upset ends and welded joints for use in drilling and operation in the oil and gas industry.

It identifies three levels of product specification such as PSL-1, PSL-2 and PSL-3. The requirements for the PSL-1 group form the basis of this standard. The PSL-2 level represents more stringent requirements in addition to the PSL-1 requirements. Level PSL-3 – additional one to the first two levels.

The international standard 5DP covers the following classes of drill pipe by steel grades:

- drill pipe grade E;
- high strength drill pipes of grade X, G and S.

A typical configuration of the drill pipe with an indication of its main elements and length is shown in Figure 2.

This standard does not consider the operational conditions of drill pipes.

Drill Stem Regulations

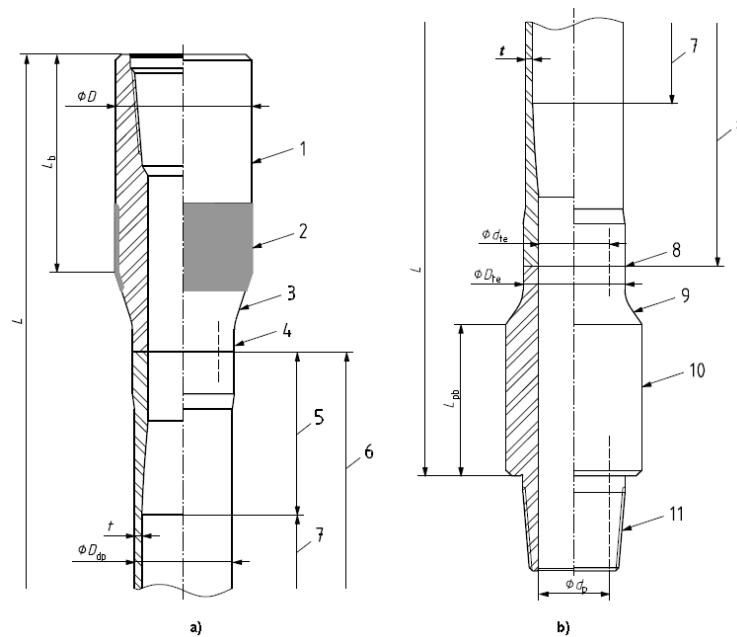


Figure 2: Drill pipe. 1 – tool-joint box; 2 - wear-resistant coating (optional); 3 - shoulder for the elevator; 4 - weld of the coupling; 5 - planted end; 6 - pipe body; 7 - pipe body; 8 - pin weld; 9 - pin socket; 10 – tool-joint pin; 11 - rotary shouldered connection.

- ØD_{dp} – outer diameter of the pipe body;
- ØD – outer diameter of the coupling;
- Ød – internal diameter of the nipple;
- ØD_{te} – the outer diameter in the weld zone;
- Ød_{ie} – the inner diameter in the weld zone;
- L_b – the outer length of the coupling;
- t – the wall thickness.

The 5DP standard impose requirements on the drill pipe as a whole, the body of the drill pipe and the tool joints. For each of the three groups the following parameters are indicated:

- geometrics (length, diameters, wall thickness);
- material requirements (tensile strength, yield strength, hardness, Charpy impact strength, etc.);
- requirements for the production process (welding, coating of surfaces, protection of threaded connections, etc.);
- marking and documentation requirements;
- requirements for technical condition monitoring (visual inspection, wet magnetic fluorescent inspection, ultrasonic inspection) (API 2010).

The Spec 7-1 standard is mainly devoted to the same aspects that are disclosed in the 5DP standard, but they concern such elements of a drilling tool as rotary kellys of various types, mud check kelly-valves, subs, drill collars, rock cutting tools (API 2006).

The international standard Spec 7-2 is dedicated to the threaded connections of a drill stem. This includes the geometrics, thread profiles. Attention is also paid to limit loads in the process of joints make-up (API 2008).

2.2.2 DS-1 Standards

The T. H. Hill Associates Inc., providing a set of standards DS-1, consisting of four volumes, occupies one of the leaders in the field of drill stem standardization. It includes the following parts:

- Volume 1 - Drilling Tubular Product Specification;
- Volume 2 - Drill Stem Design & Operation;
- Volume 3 - Drill Stem Inspection;
- Volume 4 – Drilling Specialty Tools.

The 1st volume is an analogue of the API standards. However, the format for the presentation of all requirements, as well as their content differs significantly.

First, it introduces a division into the levels of application of the recommendations - the Standard Level and the Critical Level. The Standard Level describes the minimum requirements (usually analogous to the requirements of API standards) for a particular indicator (property), a Critical Level indent more stringent, but also necessary requirements for the same indicator. Which of the levels to follow is the manufacturer's and customer's choice.

Secondly, the authors of the standards take care of navigation between sections, instructions, tables, figures. Great emphasis is placed on color marking, which makes working with the document user-friendly.

Thirdly, the list of regulated drill stem elements is extended in comparison with API standards (Table 1). In particular, a separate group of thick-walled drill pipes (TWDP) between normal-weight drill pipes (NWDP) and heavy-weight drill pipes (HWDP) is distinguished (T. H. Hill Associates, Inc 2012).

| Product | API | | DS-1, Vol. 1 | |
|--------------------|----------|-----|----------------|----------------|
| | Spec 7-1 | 5DP | Standard Level | Critical Level |
| NWDP, grade E-75 | – | X | X | X |
| NWDP, grade X-95 | – | X | X | X |
| NWDP, grade G-105 | – | X | X | X |
| NWDP, grade S-135 | – | X | X | X |
| NWDP, grade DS-140 | – | – | X | X |
| NWDP, grade DS-150 | – | – | X | X |
| TWDP, grade S-135 | – | – | X | X |

Drill Stem Regulations

| | | | | |
|---|---|---|---|---|
| TWDP, grade DS-140 | – | – | X | X |
| TWDP, grade DS-150 | – | – | X | X |
| HWDP, common welded joint | X | – | X | X |
| HWDP, high strength welded joint | – | – | X | X |
| HWDP, high strength integral joint | X | – | X | X |
| Drill Collars | X | X | X | X |
| Non-magnetic Drill Collars | X | – | X | X |
| Subs | X | – | X | X |
| Pup joints | – | – | X | X |
| Stabilizers | X | – | X | X |
| Kellys, kelly valves and rock cutting tools | X | – | – | – |

Table 1: Drilling Tubular Products Covered by API and DS-1 Manufacturing Specifications

The 2nd volume of the DS-1 standard is devoted to the operational characteristics of the elements of the drill stem. This is one of its fundamental differences from the API regulations, where the loads taken by the drill stem in the process of well construction are not taken into account, and the design algorithms are not reflected.

A significant part of the standard is occupied by diagrams of limiting values of various loads for all steel grades and geometrical parameters. Combined loads on the pipe body and combined loads on the tool-joint are considered.

Particular attention is paid to the design of the drill string in terms of fatigue wear, which is closely related to the problem of this dissertation. The technique of Tom Hill, in fact, is unique in the field of preventing fatigue breakage of the boring tool. His approach involves a comparative design analysis of proposed drill stem candidates for exposure to fatigue wear (T. H. Hill Associates, Inc 2012).

The whole 3rd volume of the standard is dedicated to the inspection and monitoring of the drill stem elements. Not only inspection methods are described, but also detailed requirements for inspection procedures, starting with geometric calibration (gauging), ending with high-tech methods for assessing the state of the material. Moreover, a separate chapter of the standard is devoted to the analysis of emergency situations and the identification of possible causes of their occurrence (T. H. Hill Associates, Inc 2012).

The 4th volume of the standard is dedicated to special tools in drilling. Under the special tool it refers to devices, which compose with drill or casing pipes to perform certain operations or surface equipment involved in working with pipe strings. The special tool works independently and does not require additional equipment for operation, excepting mechanical activators or mud-pulse signals. There are several categories of these devices:

- geosteering and measurements (logging while drilling - LWD, measurements while drilling – MWD, positive displacement motors – PDM, etc.);
- pressure control devices on the surface (Kelly valves, annular preventer, etc.);
- pipe-handling tools (elevators, rotary bushing, tongs, etc.);
- wellbore conditioning tools (near-bit reamers, casing brushes, etc.);
- fishing tools (magnets, overshot, grabs, impression tools, etc.);
- additional tools for casing pipes (liner hanger, open hole packers, hydraulic fracturing couplings, etc.);
- cementing equipment (cementing plugs, slug catcher, float shoes, etc.);
- other tools (swivels, top drive, kelly bushing, etc.) (T. H. Hill Associates, Inc 2012).

2.2.3 NS-2 Standard

In many aspects, the NS-2 standard is comparable to the 3rd volume of the DS-1 standard. However, there are some features associated with the history of this document. The standard begins with a description of the number of emergencies that occurred on Shell Expro projects from 1992 to 1998. The basis of the work is the analysis and control of the fatigue wear of the drill stem elements.

The standard addresses issues such as requirements for monitoring, testing and repairing drilling equipment, identifying fatigue cracks at early stage of their propagation, extending the service life of products by the use of special coatings, surface treatment, and removal of residual stresses in metal (Fearnley 2003).

2.3 Russian Standards for Drill Stem Elements

The main documents in the field of drill stem standardization in the territory of the Russian Federation are state standards - GOSTs. This chapter does not highlight quite similar international ISO standards, since GOSTs are considerably based on them. In addition to state standards in the Russian industry ruling documents (RD) are used. They usually take into account operational features of a product.

In addition to the listed standards, it is necessary to consider the requirements regulated in internal documents of the PJSC Gazprom Neft.

2.3.1 State Standards of Russian Federation

For a long time, GOST R 50278-92 was a fundamental standard in the field of drill stem elements in Russia. Its full title is “Drill pipes with welded tool joints. Specification”. More than 25 years have passed since its introduction in our country. In order to

Drill Stem Regulations

improve the production technology and the quality of pipes, a new standard GOST R 54383-2011 was developed in 2011, which has become an analogue of ISO 11961-2008. And, finally, in 2014, this standard was updated to the interstate standard GOST 32696-2014 (ISO 11961-2008) "Steel drill pipes for the oil and gas industry. Specification".

This latest edition is very close to API standards in terms of content. In contrast to the 1992 edition, there is already a division into three levels of specification: PLS-1, PLS-2, PLS-3. In addition to the strength groups E, X, G, S, the D group also stands out here.

Just as in the 5DP standard, requirements of the GOST address to drill pipes in general, the body of drill pipes and tool joints. For each of three groups the following features are indicated:

- geometrics (length, diameters, wall thickness);
- material requirements (tensile strength, yield strength, hardness, Charpy impact strength, etc.);
- requirements for the production process (welding, coating of surfaces, protection of threaded connections, etc.);
- marking and documentation requirements;
- requirements for technical condition monitoring (visual inspection, wet magnetic fluorescent inspection, ultrasonic inspection) (Standard 2014).

In addition to this standard, the industry uses the following ones:

- GOST 10006-80 (ISO 6892-84) "Metal pipes. Tensile test method";
- GOST 27634-95 Welded tool joints for drill pipes. Specification;
- GOST 28487-90 Tapered thread for drill string elements. Profile. Dimensions. Tolerances;
- GOST 28548—90 Steel pipes. Terms and Definitions.

2.3.2 Guidance Document of PJSC Gazprom Neft

Trying to establish the uniform rules of drill stem elements operation, development and testing, a methodical document was created at the enterprises of PJSC Gazprom Neft. It is called "Requirements for operation and non-destructive testing procedures of drill pipes and BHA elements (HWDP, TWDP, drill collars, subs) Gazprom Neft". It is a mandatory to follow this document in all divisions and drilling contractors that carry out drilling activities at the company's facilities in Russia.

This document incorporates several of the aforementioned standards.

For example, the procedure for calculating a drill string design is built based on the "Instructions for the calculation of drill strings for oil and gas wells" (Moscow, 1997) and the "Safety Rules in the oil and gas industry" (Moscow, 2015).

The part for monitoring and inspection of drill pipes is based on the 3rd volume of the DS-1 standard. Particular attention is paid to flaw detection surveys. Flaw detection methods are presented in Table 2.

In addition, the methodical guidance includes the following chapters:

- requirements for geometrics (length, diameters, wall thickness). Including the criteria for the acceptability of used elements of the drill string;
- requirements for transportation and storage of drill pipes and BHA components (HWDP, TWDP, drill collars, subs);
- requirements for the preparation and acceptance of pipes and subs on the rig;
- marking and documentation requirements;
- requirements for the use of thread lubricants (PJSC Gazprom Neft 2016).

| Name of Method | What is Done | What is being evaluated |
|----------------------|--|---|
| 1. Visual control | Full length visual examination of the inside and outside surfaces of used tubes | Straightness, mechanical or corrosion damage, debris such as scale or drilling mud |
| 2. OD gage tube | Full length mechanical gaging of the outside diameter of used drill pipe tubes | Diameter variations caused by excessive wear or mechanical damage, expansions caused by string shot, reductions caused by overpull |
| 3. UT wall thickness | Wall thickness is measured around one circumference of the drill pipe tube using an ultrasonic thickness gage | Tube wall thickness below the specified acceptance limits, minimum cross-sectional area of the tube |
| 4. Electromagnetic | Full length scanning (excluding external upsets) of drill pipe tube using the longitudinal field (transverse flaw) buggy type unit | Flaws such as fatigue cracks, corrosion pits, cuts, gouges, and other damage that exceed the specified acceptance limits |
| 5. MPI slip/upset | Examination of the external surface of drill pipe and HWDP upsets and slip areas, and HWDP center pad using the active-field AC yoke dry visible magnetic particle technique | Flaws such as fatigue cracks, corrosion pits, cuts, gouges, and other damage that exceed the specified acceptance limits |
| 6. Visual connection | Visual examination of connections, shoulders, and tool joints and profile check of threads, measurement of box swell | Handling damage, indications of torsional damage, galling, washouts, fins, visibly non-flat shoulders, corrosion, weigh/grade markings on tool joint and pin flat |

Drill Stem Regulations

| | | |
|------------------------------------|--|---|
| 7. Dimensional | Measurement or Go-No-Go gaging of box OD, pin ID, shoulder width, tong space, box counterbore | Torsional capacity of pin and box, torsional matching of tool joint and tube, adequate shoulder to support makeup stresses, adequate gripping space for tongs |
| 8. Wet visible contrast inspection | Examination of the external surface of drill pipe and HWDP upsets and slip areas, and HWDP center pad using wet visible contrast technique with an active AC or DC field | Flaws such as fatigue cracks, corrosion pits, cuts, gouges, and other damage that exceed the specified acceptance limits |

Table 2: Inspection Methods Covered by this Guidance Document (T. H. Hill Associates, Inc 2012)

2.4 Chapter Summary

Thus, it can be concluded that the obligatory state standards of Russian Federation (GOST) comply with international requirements (API) in the field of drill stem standardization. However, neither include the operational features of a particular element.

To date, the DS-1 standard is a significantly different collected volume of regulations and recommendations in this sphere.

A methodical document was created at the PJSC Gazprom Neft enterprise on the basis of state and international standards, seeking to combine key aspects of inspection and operation of drill stem, which is the right decision on the way to improve drill stem elements performance. However, it is still not enough to regulate the operational features of drill stem. Factors such as vibration, drill string buckling, dangerous combination of DLS and tensile loads that are extremely damaging to the state of the drill stem are not specified.

As one of the good examples for possible improving such standard is the NS-2 standard, which is based on a historical analysis of accidents in a particular company. It is few and far between to find a similar approach of accidents analysis, when problem solving procedure spirals into creation of a standard.

Chapter 3 Field Data Analysis

Prior to failure analysis at the facilities of PJSC Gazprom Neft, it makes sense to review the field data, as well as to identify the main requirements for drilling operations in the East Messoyakha field. For these purposes, technical project documentation and work programs for various types of drilling operations were used.

3.1 General Overview

Though the East Messoyakha field (Figure 3) was explored back in 1990's, its development was postponed as the area was lacking the transport infrastructure. This is the northernmost of the existing developed oil fields in Russia on land. Therefore, the commercial production started there only in 2016.

The license for exploration and development of the field is owned by Messoyakhaneftegaz JSC - a joint venture of Rosneft Oil Company and Gazprom Neft PJSC. However, the operational management of Messoyakhaneftegaz is carried out by Gazprom Neft.



Figure 3: A Gazprom Neft production cluster in the north of the Yamalo-Nenets Autonomous Region (PJSC Gazprom Neft 2015)

Oil production at the East Messoyakha field is conducted using horizontal wells with a horizontal length of about 1 thousand meters. The reason for this lies in the geological structure of oil facilities, complicated by a thick gas cap. Moreover, oil deposits located on different layers are separated and have different origins.

Since the occurrence of the vertical depth of these wells is one of the shallowest in the world (about 850 meters), in order to increase the drainage rate of more complex overlying layers, the wells are built using multilateral fishbone wells. It is a well design in which several branches ("ribs") are drilled from the main horizontal wellbore ("backbone"), which allows you to cover simultaneously reserves at various depths (Oil and Capital Journal 2017).

3.2 Lithostratigraphic Characteristics of the Deposit

The Cenomanian strata, where the main oil-bearing pay of the East Messoyakha is located, is considered to be very difficult to develop. In addition to permafrost, almost all known challenges in geology are concentrated there. Oil interlayers have a pronounced heterogeneity. There is a gas cap of great thickness on top of them, below the underlying water. Oil is very viscous. Moreover, low reservoir temperature (only 16°C) complicates the situation. It seemed almost impossible to extract such oil from the bowels of the earth without introduction of non-typical development methods.

At the very beginning of the development of the project, it was believed that engineers were dealing with a single monolithic object. However, according to the results of geological studies, it became clear that the main object is divided into three cyclites, which differ significantly from each other in properties and require an individual approach (Oil and Capital Journal 2017).

Stratigraphic and lithological characteristics of the deposit are presented in Table 3 and Table 4.

| TVD, m | | Stratigraphic unit | | Formation dip | | Cavernosity ratio (weighted mean value) |
|--------|--------|--|------------|---------------|-----|---|
| top | bottom | name | index | deg | min | |
| 0 | 200 | Quaternary + Paleogene deposits | Q+ P | - | - | 1,1-1,6 |
| 200 | 610 | Paleogene deposits + Taman deposits+ Chasel deposits (upper) | K2 | - | - | |
| 610 | 720 | Chasel deposits (lower) | K2 | - | - | 1,1 |
| 720 | 780 | Kuznets deposits | K2 | 0,5 | - | 1,1 |
| 720 | 750 | Kuznets + Gzsalin deposits | | | - | |
| 780 | 920 | Pokurskaya deposits | K2 – K1 | 0,5 | - | 1,1 |

Table 3: The stratigraphic well profile with the cavernosity ratio

| Index of stratigraphic unit | TVD, m | | Rock type: name, description (structure, composition, mineral assemblage etc.) |
|-----------------------------|--------|--------|--|
| | top | bottom | |
| | | | |

| | | | |
|-------------------|-----|-----|--|
| Q+ P | 0 | 200 | Argillo-arenaceous deposits, siltstone weakly compacted, sandy. Clays are gray and calcareous in some areas. |
| P +K ₂ | 200 | 720 | Lower part is presented by gray, opoka-like, weak-aleuritic, hydromicaceous clays Upper part is presented by interdigitation of gray clays with rare sandstones and opoka-like clays. |
| K ₂ | 720 | 780 | Interdigitation of gray clay aleurolite and sandstones with glauconite, with thin interlayers of limestone, below clay containing carbonaceous detritus, with the inclusion of fauna (remains of fish and pyritized algae) |
| K ₂ | 780 | 920 | Sandstones and siltstones interbedded with silt-clays. Sands and sandstones are gray various-grained quartz-feldspar with included lignite coal, gray clay, usually silty with a rich content of carbonized detritus, with the inclusion of siderite and pyrite grains |

Table 4: The lithological well profile

3.3 Possible Complications in Wells

This section is dedicated to the possible complications that could arise during the construction of wells at the East Mesoyakha field. They are considered from the point of view of their influence on possible accidents with a drill stem elements.

The first type of such complications are borehole walls cavings and collapses. Caving and collapse can cause drill string drag and slack off, which leads to additional loads on the drill pipes, and also require extra backreaming operations in the wellbore. According to the project documentation, intensive cavings and collapses are possible in the TVD from 0 to 390 m and from 780 to 920 m.

Possible causes of complications include:

- deviations from drilling program;
- speeding up during RIH/POOH operations;
- late reaction to the symptoms of possible problems;
- operational downtime (repairs, waiting for materials or tools);
- violation of drilling mud properties, such as density, viscosity, water loss.

The next complication is sticking. Stickings are possible along the entire length of the well from 0 to 920 m. Differential and mechanical sidewall stickings adversely affect the condition of the drill pipes, because while elimination the pipes can receive

Field Data Analysis

extreme tensile loads. Exceeding the allowable limits on tension may lead to the breakage of the drill string in the bottleneck.

Among the possible causes of sticking:

- poor hole cleaning from cuttings;
- deviation of drilling mud properties from the design ones;
- leaving the drill string in an open hole without movement for a long time when the drilling process or RIH/POOH operations are stopped.

And finally, one more problem noted in the documentation is a tight hole problem. As well as cavings and collapses, this type of complication refers to the instability of the wellbore wall. The narrowing of the well occurs due to the swelling of clays, which can cause drill string drag and slack off. This leads to additional overloads on the drill pipes, and also require extra backreaming operations in the wellbore. Moreover, intensive swelling can cause mechanical sticking.

Among the possible causes of well bore narrowing:

- a natural process of clays swelling, depending on the time of residence with water-based drilling fluids and deviations of the properties and parameters of the mud from the design ones (mainly from the value of water loss) (Projects Department of Gazprom Neft 2014).

3.4 Well Profile

As a profile of the mother wellbore, a five-interval horizontal profile was selected (Figure 4). In addition to the vertical section, there are buildup – hold – one more buildup – and tangent horizontal sections are distinguished. For the buildup sections, long radius of curvature was chosen, which has a DLS value from 0.6 to 2 deg/10 m (1-10 deg/100ft). The profiles of the main wellbore and an example of one side branches are described in Table 5 and Table 6 respectively.

| MD,m | Inclination, deg | TVD,m | HD, m | Azimuth, deg | DLS, deg/10m | Comments |
|---------|------------------|--------|--------|--------------|--------------|-------------------------|
| 0,00 | 0,00 | 0,00 | 0,00 | 0,00 | 0,000 | |
| 100,00 | 0,00 | 100,00 | 0,00 | 0,00 | 0,000 | Conductor Ø 324 mm |
| 554,15 | 23,12 | 550,00 | 30,68 | 130,50 | 1,494 | Surface Casing Ø 245 mm |
| 663,78 | 43,05 | 642,25 | 88,72 | 130,50 | 2,011 | Pump Equipment (upper) |
| 713,78 | 43,05 | 678,79 | 122,85 | 130,50 | 0,000 | Pump Equipment (lower) |
| 1275,38 | 88,56 | 825,00 | 579,53 | 98,93 | 1,880 | Production Casing |

| | | | | | | |
|---------|-------|--------|---------|-------|-------|--------------------|
| | | | | | | Ø 178 mm, T1 |
| 2273,63 | 88,56 | 850,00 | 1416,02 | 63,97 | 0,000 | Liner Ø 114 mm, T3 |

Table 5: Mother borehole profile

| MD,m | Inclination, deg | TVD,m | HD, m | Azimuth, deg | DLS, deg/10m | Comments |
|---------|------------------|--------|--------|--------------|--------------|----------------|
| 0,00 | 0,00 | 0,00 | 0,00 | 0,00 | 0,000 | |
| 100,00 | 0,00 | 100,00 | 0,00 | 0,00 | 0,000 | |
| 554,15 | 23,12 | 550,00 | 30,68 | 130,50 | 1,494 | |
| 919,87 | 77,54 | 780,22 | 296,08 | 123,23 | 1,879 | Kick-off point |
| 1239,20 | 50,00 | 920,00 | 575,64 | 116,53 | 0,862 | |

Table 6: Branch borehole profile

The 3-D profile of the borehole, including the lateral branch, is shown in Figure 5.

Additional features of well profile:

- Maximum inclination angle, deg – 88,56;
- The maximum DLS, deg/10m (deg/100ft) - 2,0 (6,2);
- Top of pay, m - 825;
- Designed deviation of borehole on the top of pay, m - 580;
- Permissible deviation of an actual top of pay entry point from the designed one (target area), m - 50 (Projects Department of Gazprom Neft 2014).

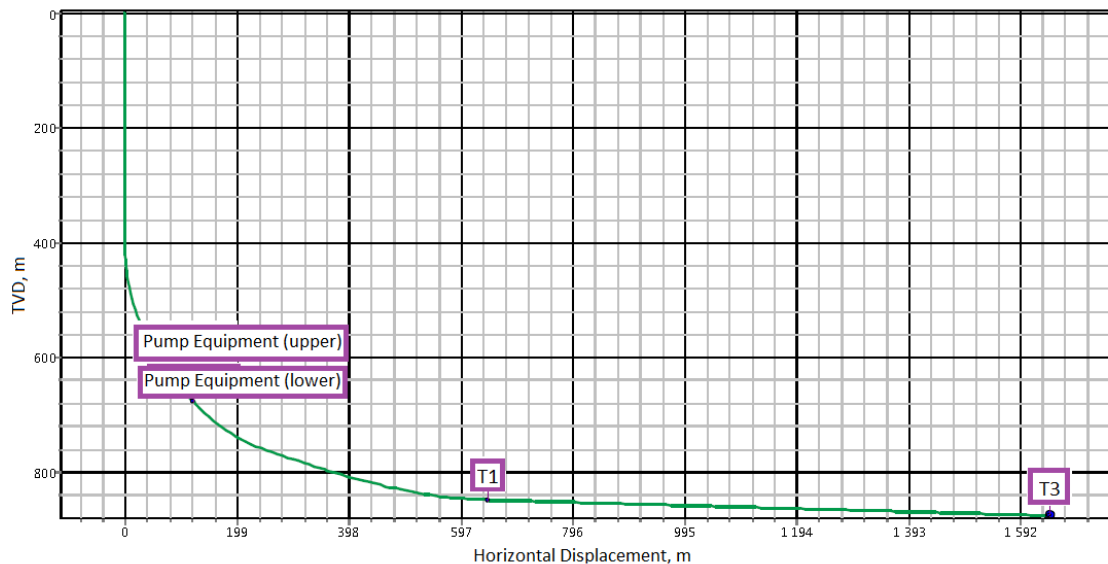


Figure 4: Well profile

Field Data Analysis

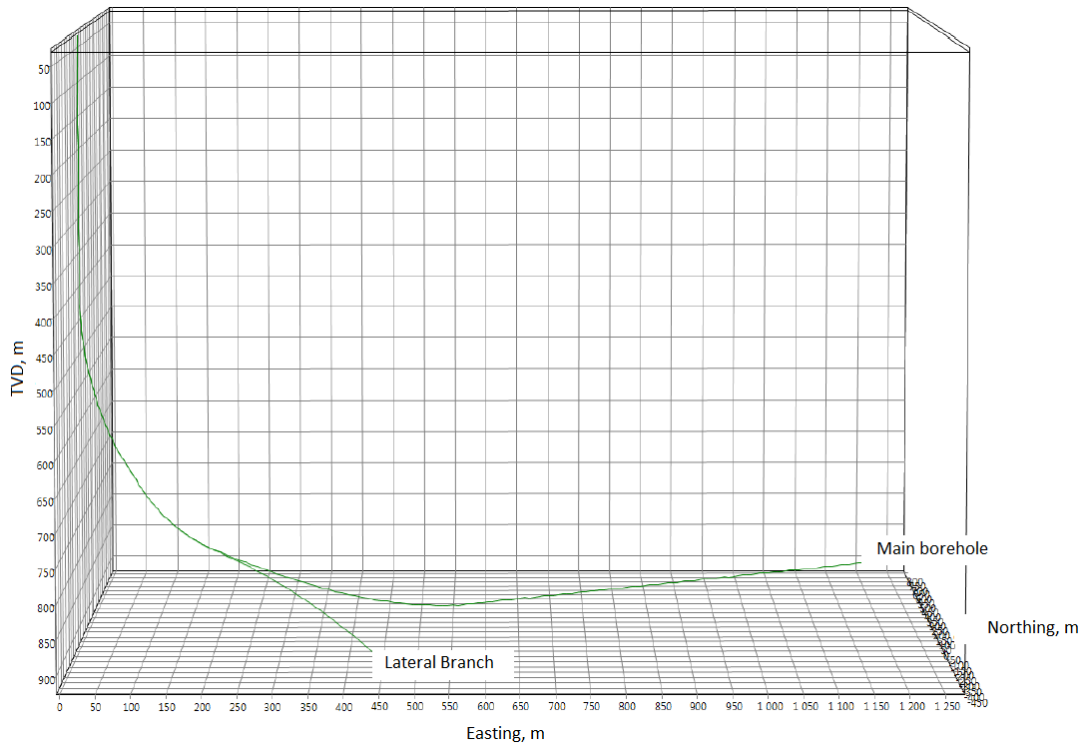


Figure 5: 3-D well profile

3.5 Used Drill String Components and Drilling Parameters

The used drill pipes and recommended drilling parameters are represented in Table 7 by intervals.

| | Drill Pipes | Drilling Method | WOB, tn | RPM | Operating Pressure, atm |
|-------------------------|-------------------------------|-----------------|------------------------|--------------------------|-------------------------|
| Conductor Ø 324 mm | HWDP-127x9.19, S-135, PREMIUM | Rotary | By drill string weight | Rotary – >80 | 51 |
| Surface Casing Ø 245 mm | NWDP 127x9,19 S-135, PREMIUM | Rotary / PDM | 8-12 | Rotary – 60-80 PDM – 230 | 120 |

Problem Description in the East Messoyakha Field

| | | | | | | | |
|---|--|-----------|------------------|-----------------|------|--------------------------------|-----|
| Intermediate Casing Ø 220,7 mm | NWDP PREMIUM | 127x9,19 | S-135, | Rotary / PDM | 8-12 | Rotary – 60 PDM – 182 | 235 |
| Production Casing Ø 220,7 mm | NWDP PREMIUM | 127x9,19 | S-135, | Rotary / PDM | 8-12 | Rotary – 60 PDM – 192 | 202 |
| Openhole Horizontal Fishbones 1-4 Ø 155,6 mm | NWDP PREMIUM HWDP-101x6,35, PREMIUM | 88,9x9,35 | G-105, S-135, | Rotary / PDM | 3-9 | Rotary – 60 PDM – 144 | 200 |
| Openhole Horizontal Fishbones 5-8 Ø 155,6 mm | NWDP PREMIUM HWDP-101x6,35, PREMIUM | 88,9x9,35 | G-105, 4145H, | RSS | 3-9 | RSS – 60-160 | 243 |

Table 7: Used drill pipes and recommended drilling parameters

3.6 Problem Description in the East Messoyakha Field

Since 2017, three drill string failures and dozens of pipe washouts were recorded at the facilities of JSC Messoyakhaneftegaz. The most problematic was the well pad, the map of which is shown in Figure 6 and described in Table 8.

It should be noted, that HWDP were predominantly washed out in the upper intervals of the drill string (it means in the zone of greater tensile load), while NWDP in the zone behind the production casing shoe in the open hole horizontal section (it means in the compression loads during drilling), which may indicate a possible negative effect of drill string buckling.

Field Data Analysis

| № | DP | Well № | TD, m | Depth from the bit, m | Depth from the surface, m | Comments |
|----|-----------|--------|--------|-----------------------|---------------------------|--|
| 1 | HWDP-88,9 | 1.1 | 2111,8 | 1291,3 | 820,5 | Thread washout |
| 2 | NWDP-88,9 | 1.1 | 1949,6 | 215,8 | 1733,2 | Pipe body washout 90 cm lower than tool joint box |
| 3 | NWDP-88,9 | 1.1 | 2012 | 562 | 1450 | Pipe body washout 20 cm lower than tool joint box |
| 4 | Jar | 1.1 | 2131 | 1400 | 731 | |
| 5 | NWDP-88,9 | 1.1 | 1971,5 | 429 | 1542,5 | Pipe body washout 26 cm lower than tool joint box |
| 6 | HWDP-88,9 | 1.1 | 1971 | 1417-1433 | 554 | Tool joint box (thread runout) |
| | HWDP-88,9 | 1.1 | | | 538 | Tool joint box (thread runout) |
| 7 | HWDP-88,9 | 1.1 | 2271,5 | 2087,5 | 184 | Tool joint box (thread runout) |
| 8 | NWDP-88,9 | 1.1 | 2445 | 1176 | 1269 | Pipe body washout 26 cm lower than tool joint box |
| 9 | NWDP-88,9 | 1.2 | 1617 | 421 | 1196 | Pipe body washout 26 cm higher than tool joint pin |
| 10 | NWDP-88,9 | 1.2 | 1348 | 568,4 | 779,6 | Pipe body washout 142 cm lower than tool joint box |
| 11 | HWDP-88,9 | 1.2 | 1738 | 1688,6 | 49,4 | Tool joint box (crosswise) |
| 12 | HWDP-88,9 | 1.2 | 1876 | 1728,1 | 147,9 | Tool joint box (crosswise) |
| 13 | NWDP-88,9 | 1.2 | 1551 | 927 | 624 | Pipe body washout 35 cm lower than tool joint box |

Problem Description in the East Messoyakha Field

| | | | | | | |
|----|-----------|-----|--------|--------|-------|---|
| 14 | NWDP-88,9 | 1.2 | 1726,4 | 1136,9 | 589,5 | Pipe body washout 58 cm lower than tool joint box |
| 15 | Jar "NOV" | 1.2 | 1979 | 1644,9 | 334,1 | |
| 16 | HWDP-88,9 | 1.2 | | | 0 | Pipe body washout 10 cm lower than tool joint box (crosswise) |
| 17 | HWDP-88,9 | 1.2 | 2074 | 1799 | 275 | Pipe body washout 10 cm lower than tool joint box (crosswise) |
| 18 | HWDP-88,9 | 1.2 | 2260 | 1621 | 639 | Pipe body washout 10 cm lower than tool joint box (crosswise) |
| 19 | HWDP-88,9 | 1.2 | 2295 | 1680,3 | 614,7 | Pipe body washout 10 cm lower than tool joint box (crosswise) |
| 20 | HWDP-88,9 | 1.2 | 2068,5 | 1813 | 255,5 | Pipe body washout 10 cm lower than tool joint box (crosswise) |
| 21 | HWDP-88,9 | 1.2 | 2129,2 | 1705,8 | 423,4 | Pipe body washout 10 cm lower than tool joint box (crosswise) |
| 22 | HWDP-88,9 | 1.2 | 2151 | 1730,6 | 420,4 | Pipe body washout 10 cm lower than tool joint box (crosswise) |
| 23 | HWDP-88,9 | 1.2 | 1927,3 | 1621,9 | 305,4 | Pipe body washout 10 cm lower than tool joint box (crosswise) |
| 24 | NWDP-88,9 | 1.2 | 2022 | 654 | 1368 | Pipe body washout 25 cm higher than tool joint pin |

Field Data Analysis

| | | | | | | |
|----|-----------|-----|--------|--------|-------|---|
| 25 | HWDP-88,9 | 1.2 | 2027,6 | 1615,5 | 412,1 | Pipe body washout 10 cm lower than tool joint box (crosswise) |
| 26 | NWDP-88,9 | 1.2 | 2052 | 617 | 1435 | Pipe body washout 63 and 68 cm higher than tool joint pin |

Table 8: Summary of washout and breakdown accidents on one of the well pads

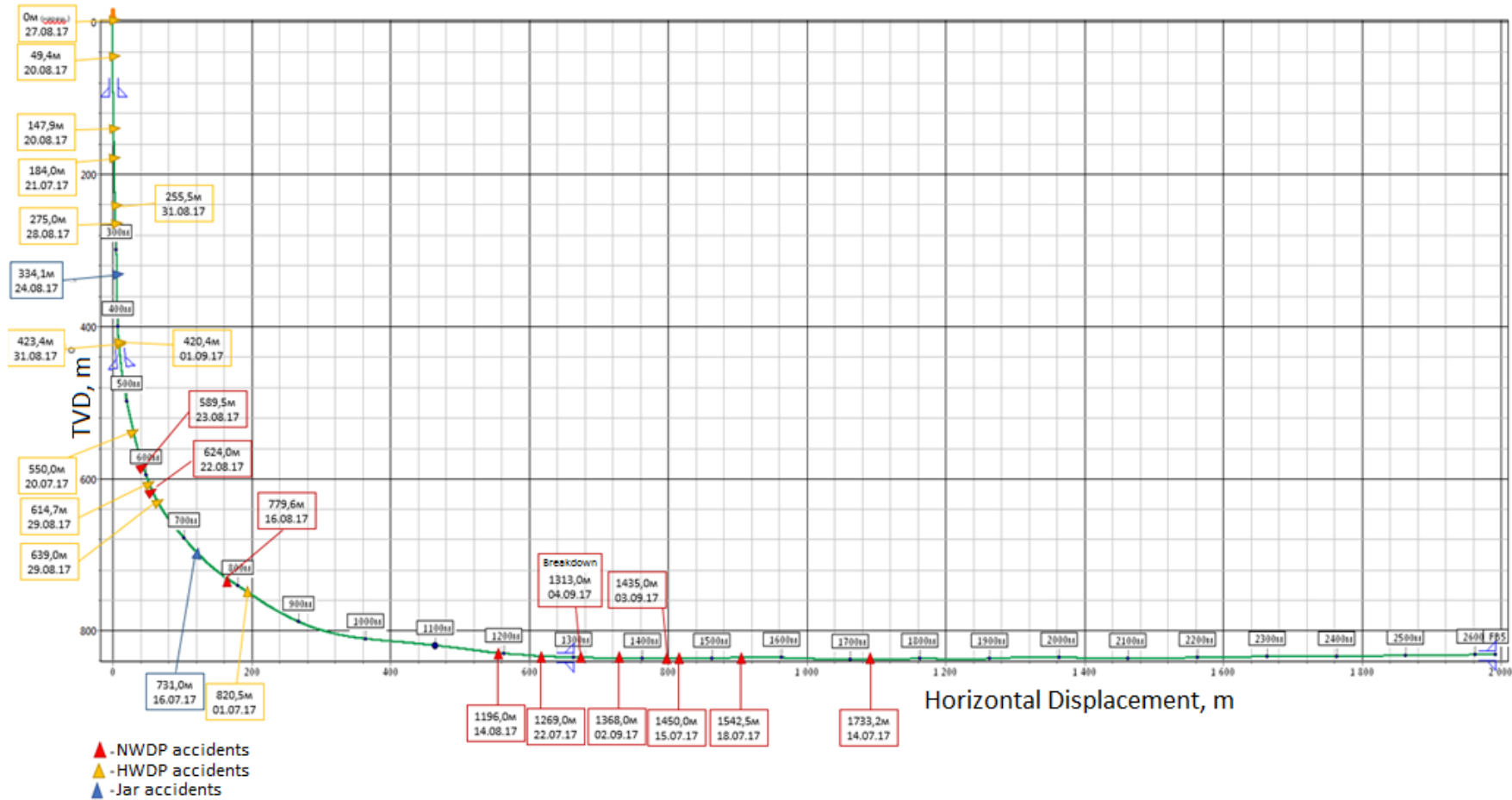


Figure 6: Schematics of washout and breakdown accidents on one of the well pads

3.7 Chapter Summary

Field data analysis showed that the East Messoyakha field is characterized by extremely difficult conditions for conducting drilling operations. The main features of wells drilling in the concerned areas:

- shallow vertical depths of the pay zones (up to 900 m) in combination with an extended horizontal part of wells (more than 1000 m);
- high values of DLS determined by the shallow vertical depth of wells;
- fishbone well design technology is chosen as the design of multilateral wells;
- high-tech equipment in the process of well construction is used (including rotary steerable systems).

The combination of all these features with the applied drilling parameters resulted in an obvious problem with the drill stem, which is inherent for this particular oil field. This problem requires careful analysis and decisions to minimize similar incidents in the future.

Chapter 4 Actual Loads Analysis Received by Drill Stem Elements During Well #1 Construction

In this and subsequent chapters, an accident case that occurred on one of the wells of the East Messoyakha field will be analyzed. Due to the privacy policy let us call this well – Well #1.

This object at the date of the accident was a multilateral well with two pilot holes, seven lateral fishbone holes and a main (mother) horizontal hole. Figure 7 shows the 3-D profile of this well.

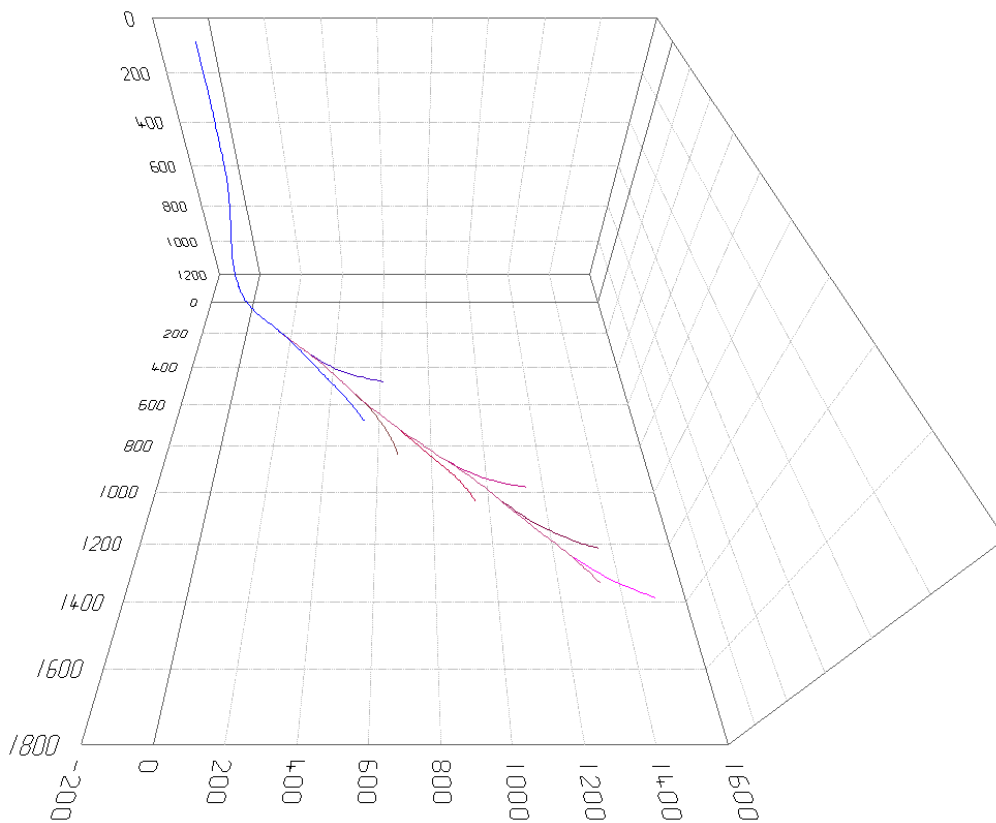


Figure 7: 3-D profile of the Well #1

Actual Loads Analysis Received by Drill Stem Elements During Well #1 Construction

4.1 Accident Description

According to the service note, during drilling the main wellbore sharp changes in the sensor readings were recorded. It happened at 9 am (local time) on June 5, 2018. Mudlogging data readings changed in the following way:

- standpipe pressure (SPP) drop from 168 to 73 atm.;
- torque values drop from 18 to 9 kN*m;
- hook load loss in off-bottom rotating mode from 51 to 46 tons.

Listed observations were confirmed after analyzing records of the mudlogging data (Figure 8).

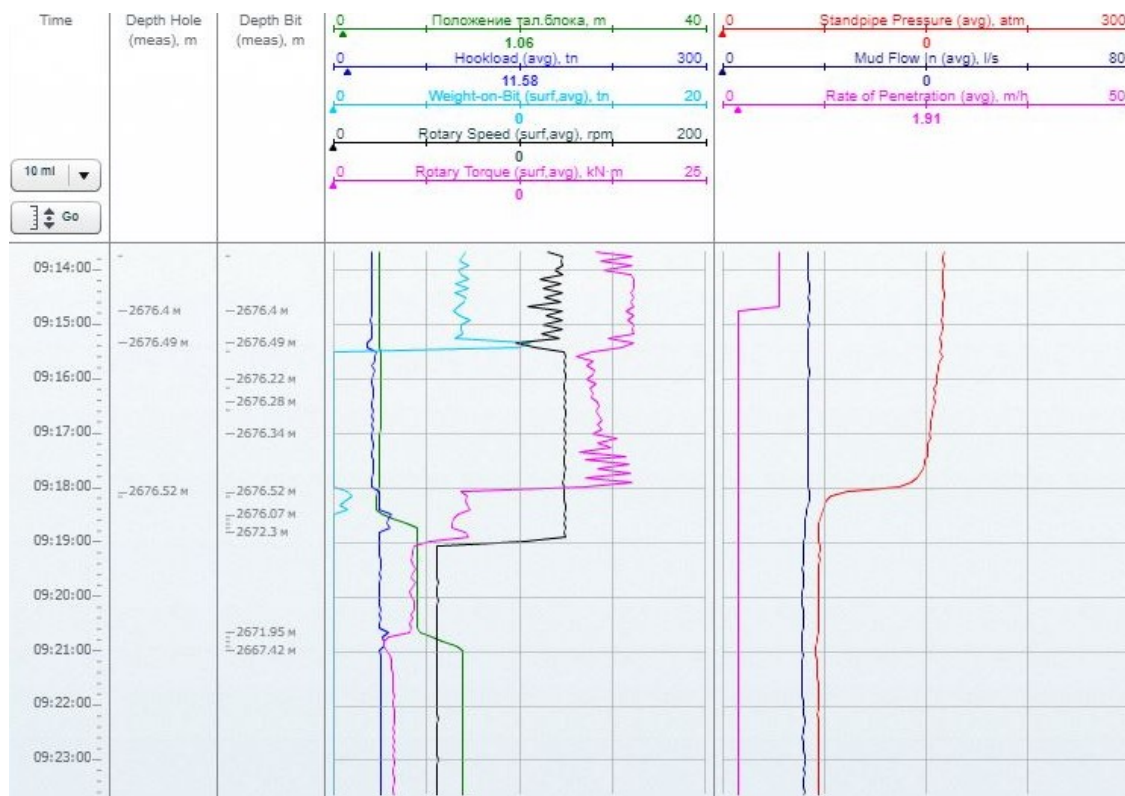


Figure 8: Mudlogging sensors readings at the moment of accident

It was decided to begin the immediate POOH operation. At 1:00 pm, when pulling out a normal-weight drill pipe, the piece of the drill pipe body was found broken at a distance of 1.62 m from the nipple of the rest part remaining in the well. 1353 m length part of the drill stem remained in the well. According to the measure of the tool, the top of the “fish” was represented by a piece of the drill pipe NWDP-88,9 x 9,35 G-105 at a depth of 1322,6 m.

Inclination angle is 89,8 ° in this interval. The production casing shoe is located at a depth of 1215 m (Figure 9). The operating time for the drill string at the time of breakdown was 286 hours.

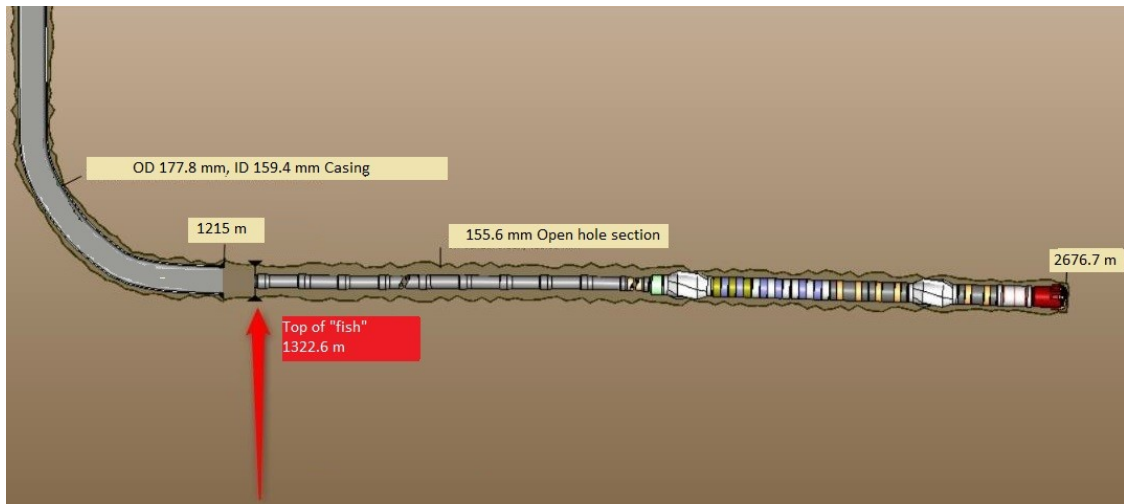


Figure 9: BHA schematics left in the Well #1

The broken drill pipe was supplied to the drilling contractor by the manufacturer “Dongying Weima Petroleum Drilling Tools Co., Ltd” (China). General information concerning a set of used drill pipes is presented in Table 9 (Dongying Weima Petroleum Drilling Tools Co., Ltd 2018).

| Pipe body | | | | | | |
|-------------------------------|----------------------|-----------------|--------------------|----------------|-----------------------|-------|
| Manufacture based on | Length, m | OD, mm | Wall thickness, mm | Steel Grade | Adjusted weight, kg/m | Class |
| API Spec 5DP | 12,25±0,15 | 88,9 | 9,35 | G-105 | 22,04 | NEW |
| Tool joint | | | | | | |
| Type | Thread hand | OD, mm | ID, mm | Shoulder | Aging | |
| Double shouldered WMDS38 | Right | 127 | 61,9 | 18° | Yes | |
| Set | | | | | | |
| Mass of the set (with TJ), tn | Number of pipes, pcs | Total length, m | Certificate № | Manufacturer | | |
| 33,21 | 123 | 1506,75 | №ZB17110403 | Dongying Weima | | |

Actual Loads Analysis Received by Drill Stem Elements During Well #1 Construction

| | | | | |
|---|--------------------------------------|-------------------------------|---------------------|--------------------------------------|
| | | | | Petroleum Drilling Tools Co., Ltd |
| Additional options | | | | |
| Hardbanding | Inner coating | Hardening | Lubrication | Protectors |
| WM8000 | WT200 | parkerising | thread-sealing | plastic with metal ring |
| Strength performance for new pipes | | | | |
| Tensile load limit for the pipe body, kN | Torque limit for the pipe body, kN*m | Torque limit for the TJ, kN*m | Makeup torque, kN*m | |
| 1692 | 35,21 | 39,59 | 23,75 | |

Table 9: NWDP-88,9 x 9,35 G-105 characteristics

Finally, after number of attempts to fish the wasted part of drill stem it was decided to leave it downhole and do sidetracking. The company took heavy losses.

4.2 Tensile Load Analysis

It is known that the main type of load affecting a drill string is an axial tensile force due to its own weight. With an increase in the mass of the suspended part of the pipes, the stresses in sections increase and may exceed the allowable limits. The highest tension is expected in the upper sections of drill string and while backreaming or POOH operation.

The value of tensile forces in pipes is influenced by the density of the pipe material. The lower the density, the longer the permissible length of the drill string. In addition to the density of the metal, the density of the drilling fluid in the well plays a significant role, since in real conditions a buoyant force also acts on a drill stem.

To comply with the limits on tensile loads, as well as for economic feasibility, the drill string is designed by several sections. In the lower part, where the mass of the suspending pipes is not great, the less durable pipes are used. The higher a considerable section, the greater the weight of a lower part, and the greater tensile loads occur in each section. If in design stage it is calculated that the loads have reached their limit values, a section with more durable pipes is to be included to the drill string. The increase in strength can be reached by an increase in wall thickness, in the diameter of pipes, a transition to a higher strength group or by several methods listed above simultaneously (Aizupe and Polyachek 2012). In our case multisection

drill string was used too. The general properties of BHA and drill string are presented in Table 10.

| No | Element | Length, m | Cumulative length, m | OD, mm | Element weight, tn | Cumulative weight, tn |
|----|---|-------------|----------------------|--------|--------------------|-----------------------|
| 1 | PDC 155,6 BT 516 US 195 | 0,32 | 0,32 | 155,60 | 0,09 | 0,09 |
| 2 | GeoPilot 5200 151 | 4,98 | 5,30 | 151,10 | 0,34 | 0,43 |
| 3 | PWD | 2,81 | 8,11 | 120,70 | 0,01 | 0,44 |
| 4 | Stabilizer | 109,00 | 117,11 | 142,90 | 0,07 | 0,50 |
| 5 | Resistivity meter SPWR | 10,17 | 127,28 | 89,00 | 0,20 | 0,70 |
| 6 | Density and porosity meter | 7,74 | 135,02 | 120,00 | 0,58 | 1,28 |
| 7 | Non- magnetic Drill Collar 90x56 | 3,41 | 138,43 | 90,00 | 0,31 | 1,59 |
| 8 | Stabilizer 149,2 | 1,72 | 140,15 | 149,20 | 0,11 | 1,71 |
| 9 | Sub | 0,78 | 140,93 | 121,00 | 0,00 | 1,71 |
| 10 | HWDP-88,9 x 15,9 | 97,21 | 238,14 | 88,90 | 2,82 | 4,53 |
| 11 | NWDP-88,9 x 9,35 | 1490,9 4 | 1729,08 | 88,90 | 33,10 | 37,63 |
| 12 | HWDP-88,9 x 15,9 | 386,18 | 2115,26 | 88,90 | 11,20 | 48,82 |
| 13 | Jar Super Bowen | 8,40 | 2123,66 | 121,00 | 0,20 | 49,02 |
| 14 | HWDP-88,9 x 15,9 | 56,18 | 2179,84 | 88,90 | 1,63 | 50,65 |
| 15 | HWDP-101,6 x 18,3 | 717,00 | 2896,84 | 102,00 | 40,15 | 90,81 |

Table 10: Drill stem used in Well #1

Safety rules in the oil and gas industry determine the values for safety factors. The safety factor of a drill string under an axial tensile load, torque, and bending load must be at least 1.5 for rotary and turbine drilling. Taking this safety factor for analysis, let's plot the distribution of limiting loads for each element of the drill stem along the entire

Actual Loads Analysis Received by Drill Stem Elements During Well #1 Construction

length (Figure 10). So, for example, according to the Table 9 allowable tensile load on the body of a broken pipe is 1692 kN. Taking into account the safety factor:

$$Q_t = Q_0 * k_t = \frac{1692 \text{ kN}}{1,5} = 1128 \text{ kN};$$

$$m_t = \frac{Q_t}{9,81} = \frac{1128 \text{ kN}}{9,81} = 115 \text{ tn}$$

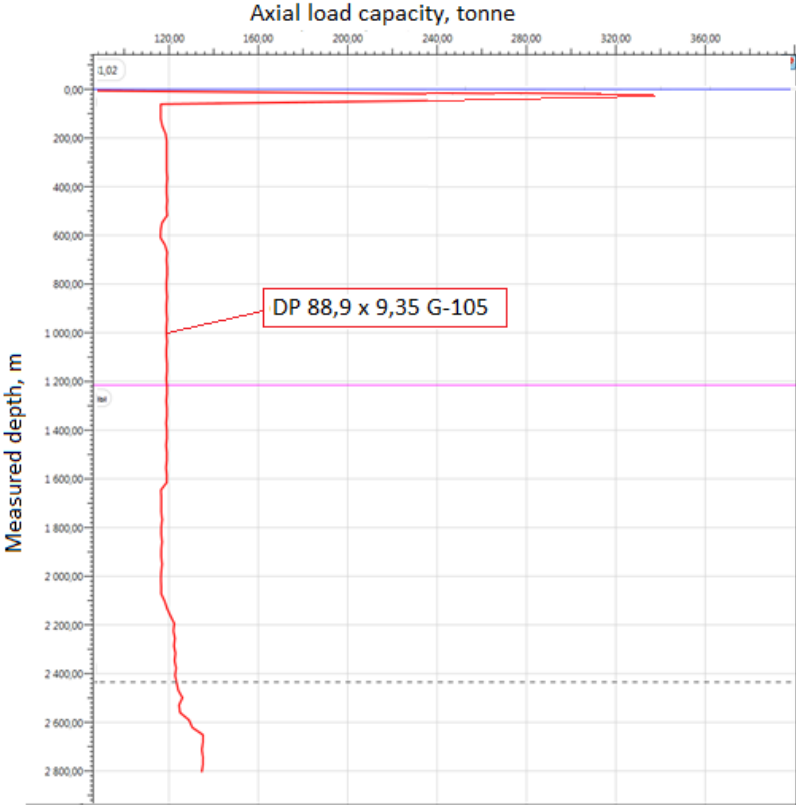


Figure 10: Limiting tensile loads along the drill stem in Well #1 while main wellbore drilling

The maximal values of hook load were identified in each branch stage by using mudlogging data sheets. This values were usually recorded while POOH with drill string drag effect. However, no overloading along the string was found. Summary about all branches is presented in Table 11. One of the columns is dedicated to the loads in broken section of drill string. Calculations are made by Landmark WellPlan software. There are no values for the first three fishbone due to the fact that the broken pipe didn't work in that branches.

An example of actual values and maximal allowable values comparison is shown in Figure 11. The blue dot indicates an actual maximal value of tensile load.

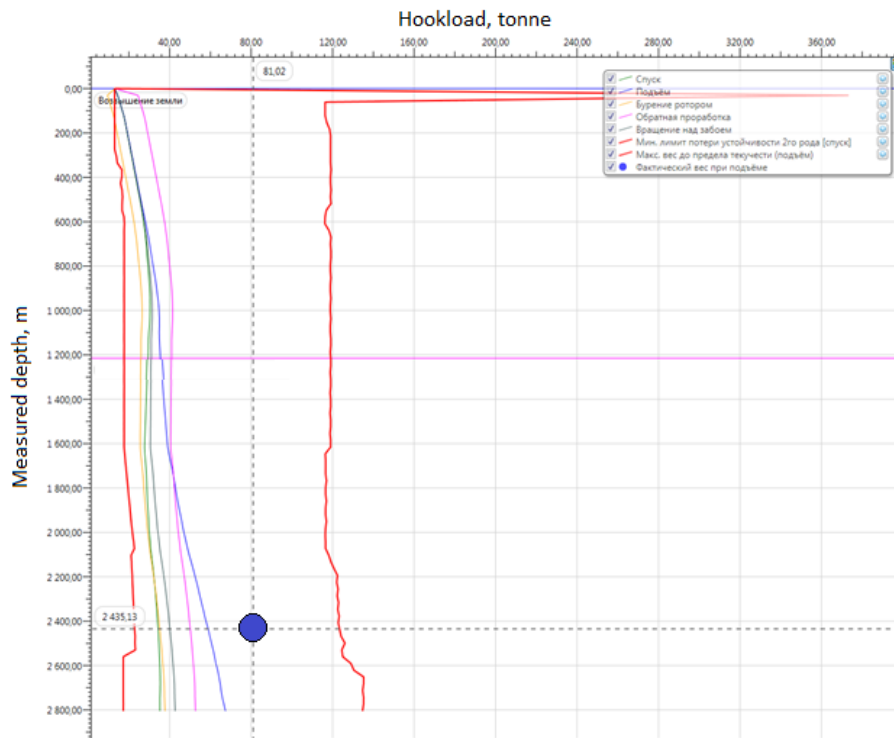


Figure 11: Tensile load distribution during different operations

| № | Bit depth, m | Operation | Time | Maximal hook load, tn | Tensile load on NWDP 88,9 x 9,35 G-105, tn | Safety margin |
|-------|--------------|-----------|------------------------|-----------------------|--|---------------|
| FB №1 | 1760,2 | POOH | 20.05.2018 6:38:47 | 57,1 | – | – |
| FB №2 | 1785,8 | POOH | 20.05.2018 16:09:43 | 59,1 | – | – |
| FB №3 | 1855,2 | POOH | 23.05.2018 7:45:19 | 63,8 | – | – |
| FB №4 | 1966,6 | POOH | 23.05.2018 15:34:14 | 62,9 | 48,5 | 2,37 |
| FB №5 | 2242,1 | POOH | 30.05.2018 16:41:15 | 60,1 | 38,1 | 3,01 |
| FB №6 | 2439,0 | POOH | 01.06.2018 13:04:20 | 75,6 | 48,7 | 2,36 |
| FB №7 | 2436,2 | POOH | 01.06.2018 13:07:49 | 81,2 | 54,0 | 2,13 |
| Main | 2665,4 | POOH | 05.06.2018 8:01:22 | 56,4 | 17,2 | 6,69 |

Table 11: Maximal tensile loads received by drill stem in all branches of the Well #1

Actual Loads Analysis Received by Drill Stem Elements During Well #1 Construction

The length of NWDP 88,9 x 9,35 G-105, used in the first three fishbone, is 856 meters. According to the fact that during the construction of single well, pipes always run in hole in the same order, it can be concluded that the broken pipe was not included to the drill pipe section for the first three fishbone construction.

The length of NWDP 88,9 x 9,35 G-105 became 1,491 meters starting from the 4th fishbone.

4.3 Torque Analysis

The excess of torsional stress in drill pipes can cause accidents while drilling in rotary mode. A failure due to torque limits exceedance is usually easy to recognize: it passes at an angle of 45 ° to the pipe axis. In our case, the fracture zone is inclined to the plane of the pipe cross-section at an angle of approximately 30° (Figure 12).



Figure 12: The photo of broken drill pipe (NWDP 88,9 x 9,35 G-105)

One of the key aim of drill string rotation is to bring the energy to the bit. Thus, it is necessary to overcome the resistance to rotation, which is associated with friction of the drill string against the borehole wall. Obviously, the maximum torque appears in the upper section of the drill string, decreasing with depth.

The torque analysis was made to identify the maximum values of the rotary table torque and to simulate the torque that occurred in each section of the wellbore up to the bottom. Afterwards the calculated values were compared with the maximum allowable values (the safety factor was taken as $n = 1$).

For the broken drill pipe, the allowable make-up torque is 23,75 kN*m (Table 9). An example of such comparison is shown in Figure 13, where the torque distribution is reflected while main horizontal borehole construction. The actual maximal value obtained from the mudlogging station readings – 20,3 kN*m was taken as the maximum rotary table torque. Summary for all branches is presented in Table 12.

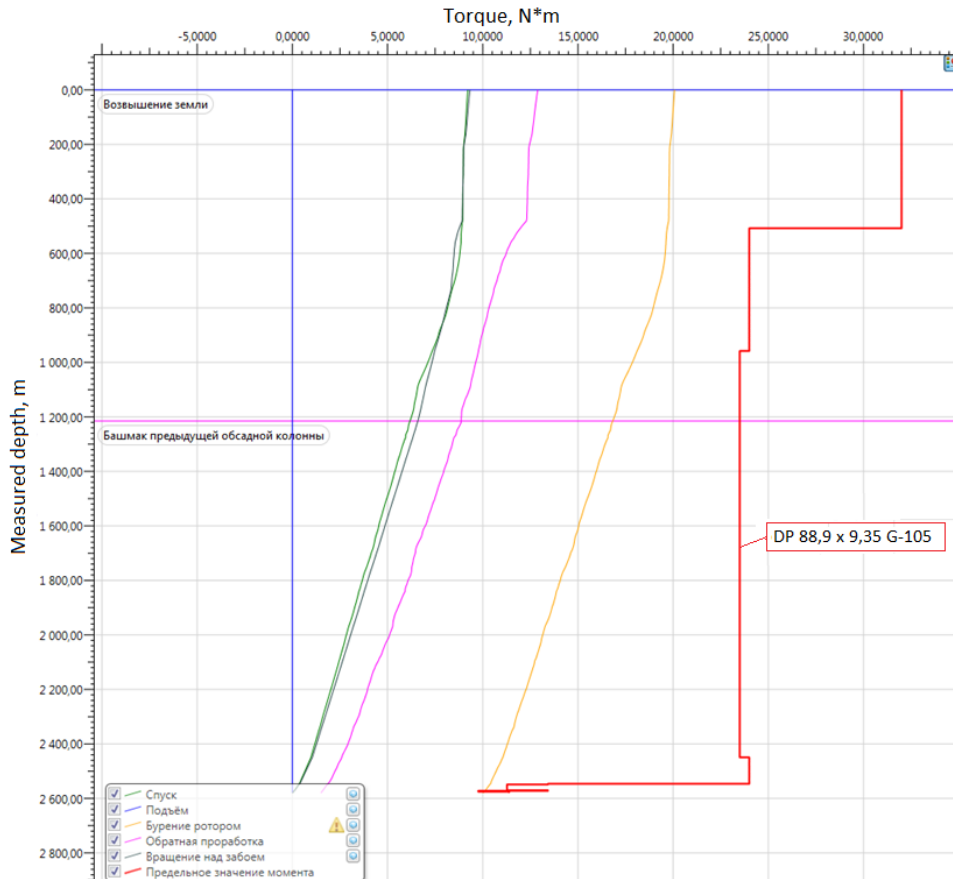


Figure 13: The torque distribution along the string in the main hole of Well #1

| | Operation (bit depth) | WOB, tn | Maximal rotary table torque, kN*m | Torque on NWDP 88,9 x 9,35 G-105, kN*m | Safety margin | Comments |
|-------|--------------------------------|------------|---|--|------------------|----------|
| FB №1 | Rotary drilling (1510 m) | 3-5 | 10,59 | – | – | – |
| FB №2 | Rotary drilling (1660 m) | 7 | 10,41 | – | – | – |
| FB №3 | Rotary | 4-5 | 16,42 | – | – | – |

Actual Loads Analysis Received by Drill Stem Elements During Well #1 Construction

| | | | | | | |
|--------------|--------------------------------|-------|-------|-------|------|--|
| | drilling (1710 m) | | | | | |
| FB №4 | Rotary drilling (1752 m) | 5-6 | 10,77 | 9,80 | 2,42 | – |
| FB №5 | Rotary drilling (2360 m) | 8-9 | 15,98 | 11,23 | 2,11 | – |
| FB №6 | Rotary drilling (2560 m) | 7-8,5 | 21,24 | 16,74 | 1,41 | – |
| FB №7 | Rotary drilling (2680 m) | 7-8,5 | 21,62 | 15,86 | 1,48 | – |
| Main | Rotary drilling (2610 m) | 6-7,5 | 20,30 | 16,2 | 1,46 | Was recorded immediately prior to the accident Not significant overload on the sub |

Table 12: Maximal torque values received by drill stem in all branches of the Well #1

4.4 Buckling Analysis

The loads acting on the drill string in horizontal wells have their own features. If the part of the string located in the vertical and curved section it is under different types of static loads, then in the horizontal section the string lies on the borehole wall and does not receive tensile forces. Thus, implementation of the weight on bit and pushing the string forward should be done by part of the pipes weight outside the horizontal interval. In this case, in a horizontal section the string is under compressive loads. Upon reaching a compressive load of a certain value, a buckling occurs (Aizupe and Polyachek 2012).

By definition, buckling is an axial compression with a lateral displacement of the drill string as a result of the destabilizing force being exceeded over the forces that keep the string in balance. The geometrical characteristics and DLS of the wellbore are two key

factors that influence whether a pipe will be buckled under axial compression and where exactly a buckling will occur (T. H. Hill 1998).

Regardless of the type (sinusoidal or helical), according to describing equations, buckling is a function of the following variables:

- **E** and **I** - Young's modulus and moment of inertia (the quantity characterizing the rigidity of a cylindrical body). A stiffer body is more resistant to buckling. Stiffness increases with increasing outer diameter of the pipe;
- **w** is the weight of pipes in drilling fluid. Mostly, the greater the weight, the less the body tends to lose stability. However, at the same time, greater weight creates greater frictional forces, which leads to an increase in compressive loads and, consequently, an increase in the probability of buckling;
- **θ** is the average wellbore inclination. The angle θ is used in buckling calculations. For vertical wells ($\sin 0^\circ = 0$), the critical load on the bit is equal to 0. As the inclination angle increases, the buckling resistance increases, however, as in the previous point, a larger angle creates larger friction forces, which leads to an increase in the probability of buckling;
- **R** is the radius of curvature of the wellbore section. Buckling is less likely at curved intervals;
- **r** is the radial clearance between the borehole wall and the pipe. Large annular gaps lead to a greater tendency for buckling, since the tubular element in this case is less restricted in the wellbore.

Buckling is divided into sinusoidal and helical (Figure 14). Sinusoidal buckling occurs relatively smoothly. The pipes gradually begin to take a sinusoidal shape, which leads to a loss of the load on the bit. The helical buckling occurs in the well more suddenly, forming spring-shape bending of the drill pipe. In this case, loading the bit becomes extremely difficult, as the drill string begins to act as a set of anchors biting the borehole wall (Mims M. 2003).

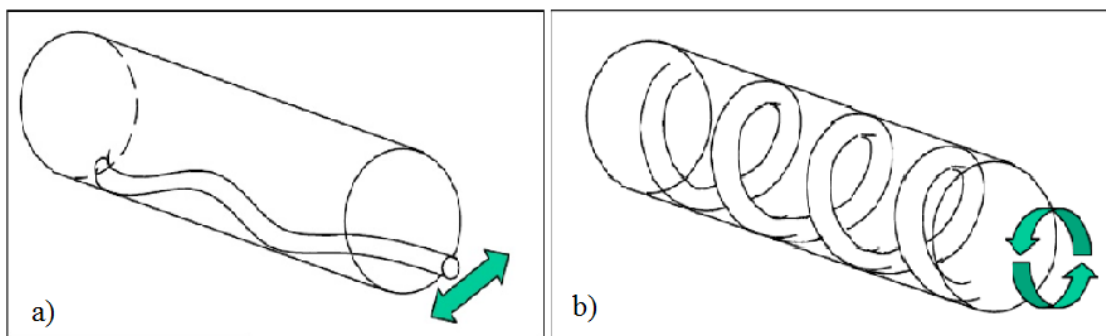


Figure 14: Buckling schematics: a) Sinusoidal, b) Helical.

For both sinusoidal and helical, the buckling itself is not critical to the drill string if there is no pipe rotation. The buckling stresses are usually well below the yield strength of the pipe. The only exception would be relatively small pipe in big hole.

However, it is crucial that you do not start rotation of the drill string until all of the pipe buckling has been released of the string. Buckled pipe will quickly be damaged if

Actual Loads Analysis Received by Drill Stem Elements During Well #1 Construction

rotated (fatigue due to the cyclic stresses). This is a significant issue for very long ERD wells, where the pipe stretch is considerable. And for sure it can be one of the reasons of occurring accidents in the East Messoyakha field.

After makeup connection, it is good drilling practice to pick-up off-bottom and release the compression out of the string prior to going back to bottom and drilling further. If the pipe stretch is significant, the compression in the pipe may not be able to be take down, as the string cannot be picked up high enough. This translates to the drill string fatigue and in some point premature fatigue cracks in the material may occur. That is why the height of the derrick should be enough to pick-up the string for buckling releasing.

Buckling is most common in the following intervals of the well path (Figure 15):

- The vertical section of the drill string is prone to buckling if in compression. This is because of the fact that the pipe in this section has no constrain and has no support from the wellbore wall, as is the pipes in the curved section of the well;
- At the beginning of extended tangent intervals. The compression in the string can be high as the pipe is pushed into the hole;
- Buckling is tend to occur above any liner top that is set deep in the well, especially if smaller diameter drill pipe is used for drilling inside the liner (for example 3½-inch drill pipe inside 7-inch liner). At least two scenarios must be allowed for, with possible intermediate points in between:
 - During drilling in sliding mode immediately next to the liner shoe. This situation will have the longest interval of small diameter drill pipe inside the large casing above top of liner.
 - During slide drilling at total depth. In this context, the small drill pipe is almost completely within the liner and, therefore, well confined. But the small drill pipe will be quite compressed because of the horizontal interval and although a true buckling may not develop inside of the liner, the area on liner top that is not as well confined will be tended to severe buckling.
 -
- Large diameter intervals may have tendency to buckling, such as deep high angle surface casing holes, or riser strings in deep-water wells.
- Buckling is unlikely (but still possible) to occur in the actual build and turn sections. This is due to the fact that drill pipes which are in bending are more resistant to buckling (Mims M. 2003).

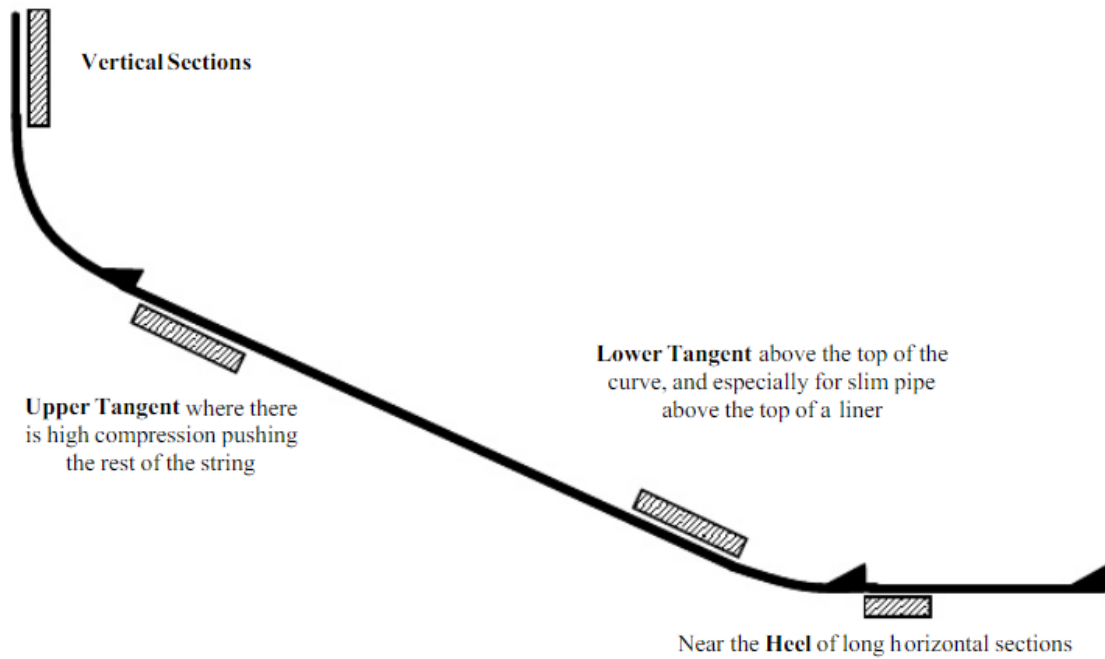


Figure 15: Sections where buckling is most likely to occur

It should be noted that the drill pipe failure occurred directly at the beginning of the horizontal section of the main wellbore in Well #1. (Figure 9).

Since during the most of the time drill stem worked in the horizontal sections of a multilateral well, a buckling analysis was conducted concerning horizontal sections. Two approaches were used:

1. Calculation of the maximum allowable WOB values and comparison of these values with the actual ones;
2. Buckling analysis in Landmark WellPlan software.

For the calculation, we used the actual data on the geometry of the well, drill pipe and BHA, drilling mud properties. An example of the input data is given in Table 13.

| Well #1 (Main borehole) | | | |
|--|-------|---|-------|
| Hole angle above KOP, deg | 50 | Drill pipe nominal weight, lb/ft | 14,82 |
| Hole angle below tangent point (θt), deg | 90 | Length of NWDP in tangent section (Ldp), ft | 2493 |
| Hole size, in | 6,125 | Length of HWDP ($Lhwdp$), ft | 318 |
| Mud weight, ppg | 9,18 | Air weight of HWDP ($Whwdp$), lb/ft | 25,30 |
| Build rate, deg/100ft | 5,73 | Length of BHA ($Lbha$), ft | 110 |
| Drill pipe size, in | 3,5 | Air weight of BHA ($Wbha$), lb/ft | 42,46 |
| Design factor for buckling (DFb) | 1,15 | | |

Actual Loads Analysis Received by Drill Stem Elements During Well #1 Construction

| Data lookup | |
|---|-------|
| Critical buckling load in tangent section (F_c), lbs | 28325 |
| Critical buckling load above kickoff point (F_{c-kop}), lbs | 22454 |
| Weight of pipe in build section (W_{bs}), lbs | 8480 |
| Buoyancy factor (K_b) | 0,859 |
| Drill pipe adjusted weight (W_{dp}), lb/ft | 17,05 |

Table 13: Input data for buckling analysis

Despite the fact that tangent sections are horizontal, the maximum WOB and the tendency to buckling will change with depth. Therefore, in the calculations it is necessary to consider two borderline situations: at the beginning and at the end of the drilled interval. If we check the conditions of bit loading at these points, then there will be no buckling in between.

The main recommendations for drilling in a rotary mode in a horizontal section are the following:

- use at least one stand of HWDP as a transition between the BHA and drill pipes;
- do buckling analysis for the beginning and end of each bit run interval;
- the smaller of the two calculated WOB will be the maximum allowable WO;
- if more WOB required, it is necessary to include more HWDP into the buckled zone of the drill string (T. H. Hill Associates, Inc 2012).

The maximum allowable load on the bit WOB_{max1} , without buckling occurrence in the upper part of the BHA is determined by the equation:

$$WOB_{max1} = \left[F_c + (K_b * \cos \theta_t) [(L_{bha} * W_{bha}) + (L_{hwdp} * W_{hwdp})] \right] \left[\frac{1}{DF_b} \right] \quad \text{Eq. 1}$$

The maximum allowable load on the bit WOB_{max2} , without buckling occurrence above KOP is determined by the equation:

$$WOB_{max2} = \left[F_{c-kop} + W_{bs} + (K_b * \cos \theta_t) [(L_{dp} * W_{dp}) + (L_{hwdp} * W_{hwdp}) + (L_{bha} * W_{bha})] \right] \left[\frac{1}{DF_b} \right] \quad \text{Eq. 2}$$

As an example, let's define the maximum WOB for the main horizontal borehole.

Substituting the values from Table 13 into equations (1) and (2), respectively, we define:

$$\begin{aligned} WOB_{max1} &= \left[28325 + (0,859 * \cos 90) [(110 * 42,46) + (318 * 25,3)] \right] \left[\frac{1}{1,15} \right] = \\ &= 24638 \text{ lb} = 11,17 \text{ tn} \end{aligned}$$

$$\begin{aligned}
WOB_{max2} &= [22454 + 848 \\
&+ (0,859 * \cos 90)[(110 * 42,46) + (318 * 25,3) \\
&+ (2493 * 17,05)] \left[\frac{1}{1,15} \right] = 26956 \text{ lb} = 12,23 \text{ tn}
\end{aligned}$$

The smaller of the two values will be the maximum allowable WOB while drilling the considered interval. Making a calculation for all intervals of interest and identifying the real maximum WOB, recorded by the mudlogging station, we enter the results in Table 14. It should be noted that in this calculation, we are interested in rotary drilling mode only. In the sliding mode, the buckling does not have a destructive character on the elements of the drill string due to the absence of cyclic loads.

| | WOB _{max} , tn | Actual WOB _{max} , tn | | WOB _{max} , tn | Actual WOB _{max} , tn |
|-------|-------------------------|--------------------------------|-------|-------------------------|--------------------------------|
| FB №1 | 11,17 | 6,76 | FB №5 | 11,17 | 10,42 |
| FB №2 | 11,17 | 7,61 | FB №6 | 11,17 | 10,30 |
| FB №3 | 11,17 | 8,17 | FB №7 | 11,17 | 10,22 |
| FB №4 | 11,17 | 5,71 | Main | 11,17 | 9,28 |

Table 14: Summary of WOB_{max} for all Well #1 branches

Thus, according to this calculation, the maximum WOB with no buckling occurrence were not exceeded by any lateral hole of the Well #1.

As for the buckling analysis in Landmark WellPlan software, the actual values for the WOB were taken as the basis. Let's follow the procedure of analysis using the example of drilling the main wellbore. Special focus will be on the area of NWDP 88,9 x 9,35 G-105 failure.

The research algorithm is as follows:

1. The investigated lateral hole is divided into intervals of penetration. Along the certain interval, the maximum allowable WOB should be common;
2. WOB_{max} is fixed for each such interval;
3. The wellbore section of buckling occurrence is recorded for each interval.
4. The actual WOB given by the readings of the mudlogging station are compared with the established limit – WOB_{max};
5. Conclusions are made about possible buckling of the drill string.

An example of main hole buckling analysis is shown in Figure 16. A summary sheet for the whole main hole is given in Table 15.

Actual Loads Analysis Received by Drill Stem Elements During Well #1 Construction

| Buckling initiation condition: | | | | | WOB>5,91 tn |
|---|-------------------|--------------|--------------|---------|-------------|
| Depth of sinusoidal buckling occurrence, m: | | | | | 1268 |
| Depth of helical buckling occurrence, m: | | | | | no |
| Depth of broken pipe, m: | | | | | 1240 |
| Time | Measured depth, m | Bit depth, m | Hookload, tn | WOB, tn | RPM |
| 5 June 01:28:00 | 2594,03 | 2594,03 | 33,11 | 3,69 | 119,91 |
| 5 June 01:28:05 | 2594,03 | 2594,03 | 33,79 | 3,01 | 119,53 |
| 5 June 01:28:10 | 2594,07 | 2594,07 | 33,04 | 3,76 | 120,09 |
| 5 June 01:28:15 | 2594,07 | 2594,07 | 33,49 | 3,31 | 119,36 |
| 5 June 01:28:20 | 2594,1 | 2594,1 | 33,28 | 3,52 | 120,1 |
| 5 June 01:28:25 | 2594,14 | 2594,14 | 33,03 | 3,77 | 119,47 |
| 5 June 01:28:30 | 2594,17 | 2594,17 | 33,07 | 3,73 | 119,99 |
| 5 June 01:28:35 | 2594,17 | 2594,17 | 33,43 | 3,37 | 119,26 |
| 5 June 01:28:40 | 2594,34 | 2594,34 | 30,29 | 6,51 | 119,64 |
| 5 June 01:28:45 | 2594,41 | 2594,41 | 31,18 | 5,62 | 119,71 |
| 5 June 01:28:50 | 2594,51 | 2594,51 | 30,26 | 6,54 | 119,62 |
| 5 June 01:28:55 | 2594,61 | 2594,61 | 30,19 | 6,61 | 119,78 |
| 5 June 01:29:00 | 2594,64 | 2594,64 | 30,58 | 6,22 | 119,58 |
| 5 June 01:29:05 | 2594,71 | 2594,71 | 30,29 | 6,51 | 119,66 |
| 5 June 01:29:10 | 2594,78 | 2594,78 | 30,26 | 6,54 | 119,52 |
| 5 June 01:29:15 | 2594,81 | 2594,81 | 30,24 | 6,56 | 119,99 |
| 5 June 01:29:20 | 2594,85 | 2594,85 | 30,28 | 6,52 | 119,24 |
| 5 June 01:29:25 | 2594,88 | 2594,88 | 30,09 | 6,71 | 118,03 |
| 5 June 01:29:30 | 2594,88 | 2594,88 | 30,29 | 6,51 | 119,23 |
| 5 June 01:29:35 | 2594,91 | 2594,91 | 29,99 | 6,81 | 105,14 |
| 5 June 01:29:40 | 2594,91 | 2594,91 | 30,59 | 6,21 | 119,3 |
| 5 June 01:29:45 | 2594,95 | 2594,95 | 30,14 | 6,66 | 115,93 |
| 5 June 01:29:50 | 2594,95 | 2594,95 | 30,44 | 6,36 | 115,71 |

| | |
|--|-------------------------|
| | Exceeding values |
| | Values within the limit |

Figure 16: Example of the mudlogging data-sheet buckling analysis

| Drilled interval, m | WOB _{max} , tn | Sinusoidal buckling occurrence depth, m | Helical buckling occurrence depth, m | Top of broken pipe, m | Buckling time, min | Buckling percentage of total drilled time, % |
|-------------------------|-------------------------|---|--------------------------------------|-----------------------|--------------------|--|
| Well #1 (Main borehole) | | | | | | |
| 2559-2569 | 6,95 | 1238 | no | 1210 | 1,0 | 5,4 |

| | | | | | | |
|-----------|------|------|----|-----------|------|------|
| 2569-2580 | 6,98 | 1239 | no | 1220 | 0,0 | 0,0 |
| 2580-2590 | 7,04 | 1240 | no | 1230 | 0,5 | 2,3 |
| 2580-2600 | 5,91 | 1268 | no | 1240 | 25,8 | 43,2 |
| 2600-2610 | 5,31 | 1269 | no | 1250 | 2,3 | 7,4 |
| 2610-2620 | 6,27 | 1233 | no | 1260 | 0,0 | 0,0 |
| 2620-2676 | 6,90 | 1236 | no | 1270-1320 | 14,5 | 9,7 |

Table 15: Buckling time for Main borehole of Well #1

Therefore, according to the simulation in a software product, while drilling the main borehole, the drill string could experience a sinusoidal loss of stability (sinusoidal buckling) for 9,7% of the time. This is equivalent to 3140 revolutions of the drill string. It is noteworthy that the risk zone (1233–1269 m) was located very close to the broken drill pipe (1210–1320 m) operating zone.

However, it should be noted that the presented mudlogging data records concerning WOB are only rating values in each unit of time, which depends on direct measurements of the hook load. Taking these values as proposed one will not be absolute correct, but still when bringing into correlation these values with the values of ROP, it can be concluded that the real WOB and the calculated by mudlogging station correlate fairly closely. Of course, this assumption applies only to the intervals without severe slack off appearance.

Summary Table 16 for bucking analysis in boreholes of Well #1 is presented below. The first three fishbone are not taken into account because of absence of broken pipe there.

| Drilled interval, m | Sinusoidal buckling occurrence depth, m | Helical buckling occurrence depth, m | Buckling time for broken pipe, min | Buckling time, min | Buckling percentage of total drilled time, % |
|---------------------|---|--------------------------------------|------------------------------------|--------------------|--|
| Main borehole | | | | | |
| 2560-2676 | 1230-1260 | no | 29 | 44 | 9,7 |
| FB7 | | | | | |
| 2337-2790 | 1230-1260 | no | 12 | 659 | 56,5 |
| FB6 | | | | | |
| 2120-2620 | 1230-1260 | no | 48 | 479 | 33,9 |
| FB5 | | | | | |
| 1870-2364 | 1230-1260 | no | 0 | 521 | 53,4 |

Actual Loads Analysis Received by Drill Stem Elements During Well #1 Construction

| FB4 | | | | | |
|-----------|-----------|----|---|-----|------|
| 1664-2266 | 1220-1290 | no | 0 | 128 | 52.6 |

Table 16: Buckling time summary for Well #1 laterals

Thus, analyzing the five laterals of Well #1 it can be concluded that a significant part of the time broken drill pipe was working in a possible sinusoidal buckling interval 1220-1290 m. In some boreholes (FB4, FB5, FB7) this value even exceeded 50% of the total drilling time. As for the broken pipe, the estimated time of operation in the sinusoidal buckling mode was 89 minutes, or in terms of the RPM – 10,690 revolutions.

4.5 Tri-axial Loading Analysis

In 1913, the Austrian mathematician and mechanic engineer Richard Edler von Mises, together with Maximilian Huber, proposed a yield criterion that characterizes the limiting stress in the body, upon reaching which the polycrystalline will have noticeable plasticity (in our case it will be failed).

Plastic material starts to be damaged in those areas where the von Mises stress reaches the limiting values. Usually, as in this work, the yield strength of the material is used as the limiting value of the stress (Rabotnov 1962).

The von Mises equivalent stress in the body of the drill pipe σ_{vm} consists of three main stresses: radial (σ_r), axial (σ_a) and tangential (or tangential - σ_t).

$$\sigma_{vm} = \sqrt{\frac{(\sigma_r - \sigma_t)^2 + (\sigma_r - \sigma_a)^2 + (\sigma_t - \sigma_a)^2}{2}} \quad \text{Eq. 3}$$

These stresses depend on pressures in the pipe and annulus; axial compressive or tensile forces; borehole geometry and pipe geometry. The equivalent stress is such a stress, under the action of which the material in a simple tension-compression condition would be in the equally dangerous state with the combined tri-axial stress state under consideration (Figure 17).

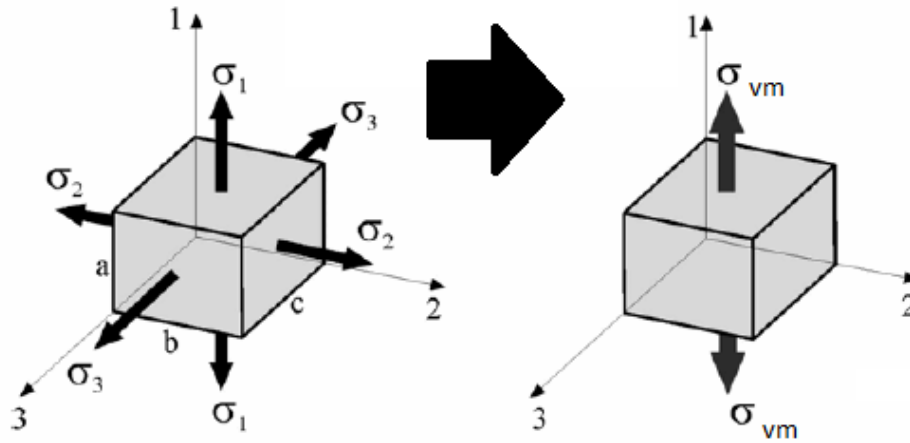


Figure 17: Tri-axial stress state transition into the equivalent stress

Assuming that radial stresses are not significant we can neglect them. The most critical for the overloading analysis are forces, which arise due to weight of metal and rotation of the string. Therefore, we come to the maximum share stress theory (Osipov 2008):

$$\sigma_{vm} = \sqrt{\sigma^2 + 3\tau^2} \quad \text{Eq. 4}$$

Let's choose the breakdown zone of drills string to analyze and as input let's take the worst-case scenario values:

- tensile loads are taken while backreaming operation;
- torque values are taken while maximum RPM rate;
- maximal DLS values are taken from the real directional drilling reports.

To calculate an axial stress we use one of the Lamé equation for axial stress (Mitchell 1995):

$$\sigma_a = \frac{T}{A_{cs}} + \sigma_{bending} \quad \text{Eq. 5}$$

where

A_{cs} – pipe cross-sectional area, in²;

T – tensile force, lbs;

$\sigma_{bending}$ – additional axial force due to bending in curved hole, psi;

and $\sigma_{bending} = \frac{F}{A_{cs}}$, where F is taken as the larger of two calculated values (Mitchell 1995):

- Beam force:

$$F_{beam} = 17,135(D)C(D^2 - d^2) \quad \text{Eq. 6}$$

Actual Loads Analysis Received by Drill Stem Elements During Well #1 Construction

- Lubinski force:

$$F_{lub} = \frac{17,135(D)C(D^2-d^2)}{\tanh\left[0,2\sqrt{\frac{T}{D^4-d^4}}\right]} \quad \text{Eq. 7}$$

where C – dogleg severity, deg/100ft.

These equations are common in drilling practice for calculating equivalent stresses in casing. To carry out a similar calculation for drill pipe, it is necessary to take into account the shear stress arising from the torque. Tangential stresses arise as a result of reacting torque arising from the downhole motor operation or, as in our case, the rotary drilling (VNIITneft 1997):

$$\tau = \frac{M}{W_p} \quad \text{Eq. 8}$$

$$W_p = \frac{\pi D_i^3 \left(1 - \frac{D_i^4}{D_o^4}\right)}{16} \quad \text{Eq. 9}$$

where M – torque at certain depth, N*m;

W_p – polar section modulus;

D_i – pipe ID, m;

D_o – pipe OD, m.

Substituting the available data into the listed equations, we find the values of the main stresses. The input and output data are presented in Table 17.

Substituting obtained values of the axial stress and tangential stress into Eq. 3 we find the equivalent stress:

$$\sigma_{vm} = \sqrt{\sigma^2 + 3\tau^2} = \sqrt{38991^2 + 3 \cdot 22145^2} = 54695 \text{ psi} = 377 \text{ MPa}$$

Let's compare equivalent stress value with the yield strength of the pipe. It is known that $\sigma_{yield} = 105000$ psi.

$$\frac{\sigma_{vm}}{\sigma_{yield}} = \frac{105000 \text{ psi}}{54695 \text{ psi}} = 1,92$$

Thus, even considering worst-case scenario for a broken drill pipe, the evaluation of the equivalent stress by von Mises showed that the limiting values for tensile loads were not exceeded. According to calculations, the safety margin for this analysis was 1,92.

| NWDP 88,9 x 9,35 G-105 | | | |
|----------------------------|----------|---------------------------------------|--------|
| Inputs | | Outputs | |
| Pipe OD, in | 3,5 | Cross sectional area, in ² | 4,30 |
| Pipe ID, in | 2,602 | Wall thickness, in | 0,449 |
| Pipe weight, lb/ft | 15,5 | Tension, lbs | 61795 |
| Grade | G-105 | Tangential stress, psi | 22145 |
| Total depth, ft | 8780 | Axial stress, psi | 38991 |
| Modulus of elasticity, psi | 30000000 | Lubinsky force, lb | 105924 |
| Depth of interest, ft | 4337 | Beam force, lb | 22017 |
| DLS, deg/100ft | 6,7 | Bending stress, psi | 24625 |
| Mud weight, ppg | 9,18 | | |

Table 17: Input and output data of tri-axial stress analysis

4.6 Chapter Summary

During analysis of actual loads received by NWDP 88,9 x 9,35 G-105 on Well #1 of East Messoyakha field several analytical calculations and observations were conducted. The results of which can be concluded as the following:

1. Tensile loads analysis illustrated the absence of the drill string tensile overloads, which can be also explained by the shallow TVD of the well and the absence of severe problems with drill stem sticking;
2. Checking for possible excess of torque in the process of drilling illustrated the absence of those in the drill string;
3. The DS-1 buckling analysis outlined the maximum allowable WOB, but this calculation is only an estimate and does not take into account many factors (for example, friction coefficients, the actual trajectory of the wellbore, etc.). According to these calculations, there was no buckling in the drill string. However, the second calculation made in the Landmark WellPlan software more significantly reduced the allowable WOB, especially in the interval of 1220-1290 m, which is very close to the the drill pipe breakage zone (1322 m). This zone (the beginning of the horizontal section) is also described in the literature as one of the potential intervals for the buckling appearance. The buckling time estimation showed that the broken pipe could have been under the influence of buckling for 89 minutes, which is equivalent to 10,690 revolutions;

Actual Loads Analysis Received by Drill Stem Elements During Well #1 Construction

4. Von Mises equivalent stress analysis showed that the allowable values for tensile loads were not exceeded even considering worst-case scenario. According to calculations, the safety margin for this analysis was 1,92.

Chapter 5 Drill Pipe Technical Expertise

Conclusions

In September 2018 a contract for drill pipe metal technical expertise was signed between Eurasia Drilling Company LLC (drilling contractor) and the New Materials Study Center on the basis of the Gubkin Russian State University of Oil and Gas (National Research University).

5.1 Subject of research and documentation review

The following pieces were presented for the study:

- one full-size fragment of the drill pipe (labeled #1): the outer surface is without visible mechanical damage with weak uniform corrosion marks, the cut of the fragment is mechanical, there are no sections of metal heating;
- one semi-cylindrical fragment of the broken drill pipe (labeled #2): the outer surface is without visible mechanical damage with weak corrosion marks, the cut of fragment is mechanical on one side, and there is a fracture zone with a crack on the other, there are no metal heating sections.

The view of the presented pipe fragments is shown in Figure 18.



Figure 18: Two pieces of broken pipe delivered for the expertise

Inspection of the damaged drill pipe showed no visible deformations along the pipe body. There were no deep cuts or corrosion damage in the fracture zone that could cause destruction. The fracture zone on the semi-cylindrical fragment #2 is inclined with respect to the cross-sectional plane of the pipe at an angle of approximately 30°. On the section of the pipe adjacent to the plane of fracture, there is a through crack.

Together with fragments of the drill pipe the following documentation was provided:

Drill Pipe Technical Expertise Conclusions

- Equipment certificate №C-2036 for a set of NWDP 88,9 x 9,35 G- 105 EU drill pipes;
- Quality certificate Dongying Wiema Petroleum Dilling Tools Co., LTD No. ZB17110403;
- Service note on the incident at the site of Messoyakhaneftgaz JSC (signed by R.N. Ivanov, Supervisor);
- accident description by chronology of work at the Well #1;
- mudlogging diagrams for the following period: 03.06.2018 - 05.06.2018.

According to the Equipment certificate №C-2036, the date set of pipes packaging is 10.01.18, the total penetration was 3069 m and 196 hours of circulation (Elagina O., Buriakin A. and Volkov A. 2018).

5.2 The purpose and order of the study

The purpose of the study was to conduct a technical expertise of steel drill pipe for compliance of the metal with the requirements of GOST and API standards; identifying possible causes of destruction.

As part of the research program, the following work was performed:

- documentation and operational history analysis;
- templates testing for compliance with certificate requirements and requirements of the standards;
- fractography studies of the fracture surface;
- the microstructure analysis in different areas of destruction;
- fatigue tests conducting to determine the number of cycles to failure with a stress concentrator samples and without (evaluation of fatigue strength at different areas) (Elagina O., Buriakin A. and Volkov A. 2018).

5.3 Verification of the chemical composition, phase structure and mechanical properties of the metal

To assess the compliance of the drill pipe metal with the requirements of the documentation, a full-size fragment No. 1 was sampled according to the Sampling Act #1 of September 24, 2018. Samples were made to analyze the chemical composition, uniaxial tension test, the impact test, structure studies, hardness measurement and cyclic-loads test.

Comparison of the obtained data on the chemical composition of the drill pipe metal showed that the analysis results comply with the requirements of API 5 DP standard and the quality certificate for the set of drill pipes №ZB17110403 (Table 18).

Verification of the chemical composition, phase structure and mechanical properties of the metal

| | Mass content, % | | | | | | | | |
|------------------------------------|-----------------|---------------|-------------------|-----------------|----------------|---------------|---------------|---------------|---------------|
| | C | Si | Mn | P | S | Cr | Ni | Mo | Cu |
| Lab studies | 0,260 | 0,256 | 1,074 | 0,0010 | 0,0105 | 0,867 | 0,124 | 0,174 | 0,056 |
| API 5DP | - | - | - | 0,020 (max) | 0,015 (max) | - | - | - | - |
| Certificate №ZB17110403 | 0,26- 0,27 | 0,24- 0,26 | 1,06 - 1,09 | 0,009- 0,013 | 0,004 | 0,88- 0,91 | 0,04- 0,11 | 0,16- 0,17 | 0,05- 0,06 |

Table 18: Comparison of chemical analysis data

Strength factors under uniaxial tension meet the requirements of API 5 DP. It should be noted that the relative elongation of the metal, measured on samples cut from fragment #1, showed values below the data of certificate № ZB17110403 almost 2 times, indicating a loss of material ductility (Table 19).

| | Strength , MPa | Yield strength, MPa | Relative extension, % | Impact energy, CV ²¹ , J | Heat treatment |
|--|---------------------------|------------------------------------|--------------------------------------|---|-------------------------------|
| API 5 DP | ≥793 | 724-931 | - | ≥38 (min for sample) ≥43 (min average for the series) | - |
| Certificate No. ZB 17110403 | 925-1033 | 817-924 | 21,6 – 24,0 | 86 89 - 133 | Quenching and tempering |
| Test results | 919 | 843 | 12,2 | 91 - 107 | - |

Table 19: Comparison of mechanical properties

The impact strength of metal, determined on K-CV type samples, is at a high enough level and meets API requirements of 5DP standard and certificate №ZB17110403. Crack initiation test performed according to fracture diagrams showed that the energy, which goes into the process of crack formation, is in the range from 14 to 25 J. It is less than 28% of the total energy of destruction. Thus, the metal of the drill pipe showed a high tendency to crack. The subsequent crack propagation goes with more significant energy absorption.

Drill Pipe Technical Expertise Conclusions

The hardness measurements made in the cross section of the drill pipe wall of the fragment #1 showed values in the range from 298 to 306 HV. Lower hardness values occur on the surface layers of the pipe wall, which indicates the absence of concentrated loads that occur on the surface of the pipe wall.

Microstructure analysis of the metal was performed on samples cut in the longitudinal and transverse sections of the wall. Photos of non-metallic inclusions and microstructure are presented in Figure 19 and Figure 20.

Metal is characterized by the presence of predominantly oxide non-metallic inclusions. Impurity rating – D 1.5. The structure of the metal wall - tempered martensite. No differences were found between the structure in the central part of the wall of the drill pipe and the near-surface layers (Elagina O., Buriakin A. and Volkov A. 2018).

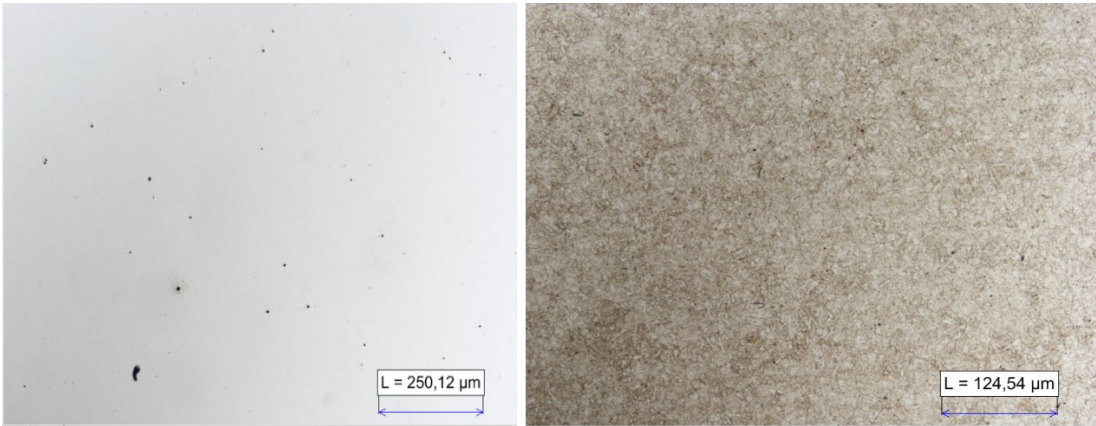


Figure 19: Longitudinal cross-section of the pipe

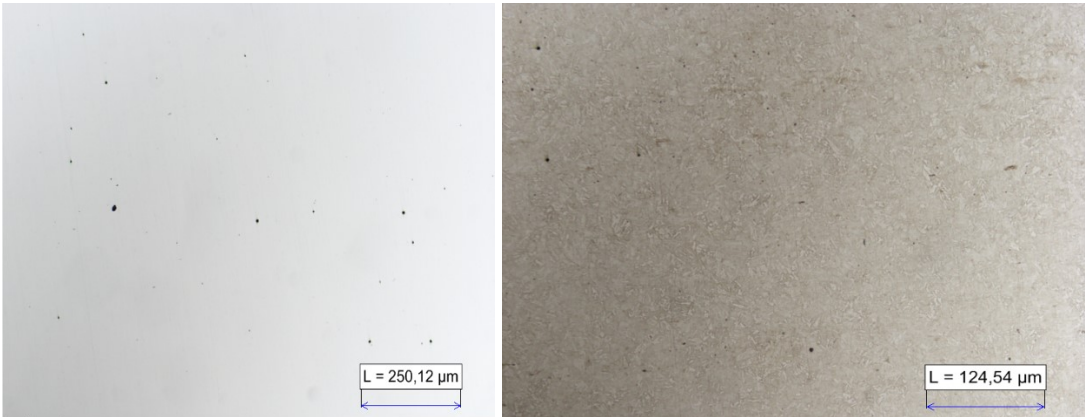


Figure 20: Lateral cross-section of the pipe

5.4 Fractography Studies

A part of the broken pipe and a photo of the fracture were presented for fractography analysis (Figure 21). The photo illustrates that the fracture surface is characterized by

the presence of two zones that differ in their relief. The characteristic washings can be detected in zone I. They form a significant relief. In the central part of zone I there is a protruding section (I.1), obliquely oriented both to the inner and outer surfaces of the pipe. It is assumed that this is the site of crack initiation. There is a ridge separating the inner part of the fracture from the outside in the center of the cross section of the pipe wall at section I.1. Judging from the photo, the fracture surface adjacent to the inner surface of the pipe at section I.1 has a small inclination angle characteristic of the initial stage of crack initiation (1st stage). The inclination angle of the fracture surface changes after the ridge by about 30-50° to the outer surface. This indicates a change in the stress state in the pipe wall as the crack develops in section I.1. The conical shape of this section indicates a significant contribution of the hydro-erosion factor to the output of the drilling fluid through the formed through crack. Probably, a crack initiation process started on the inner surface of the pipe and began to develop towards its center. As the crack grows and opens, the wedging effect of the drilling mud resulted in a change in the stress state at the crack tip.

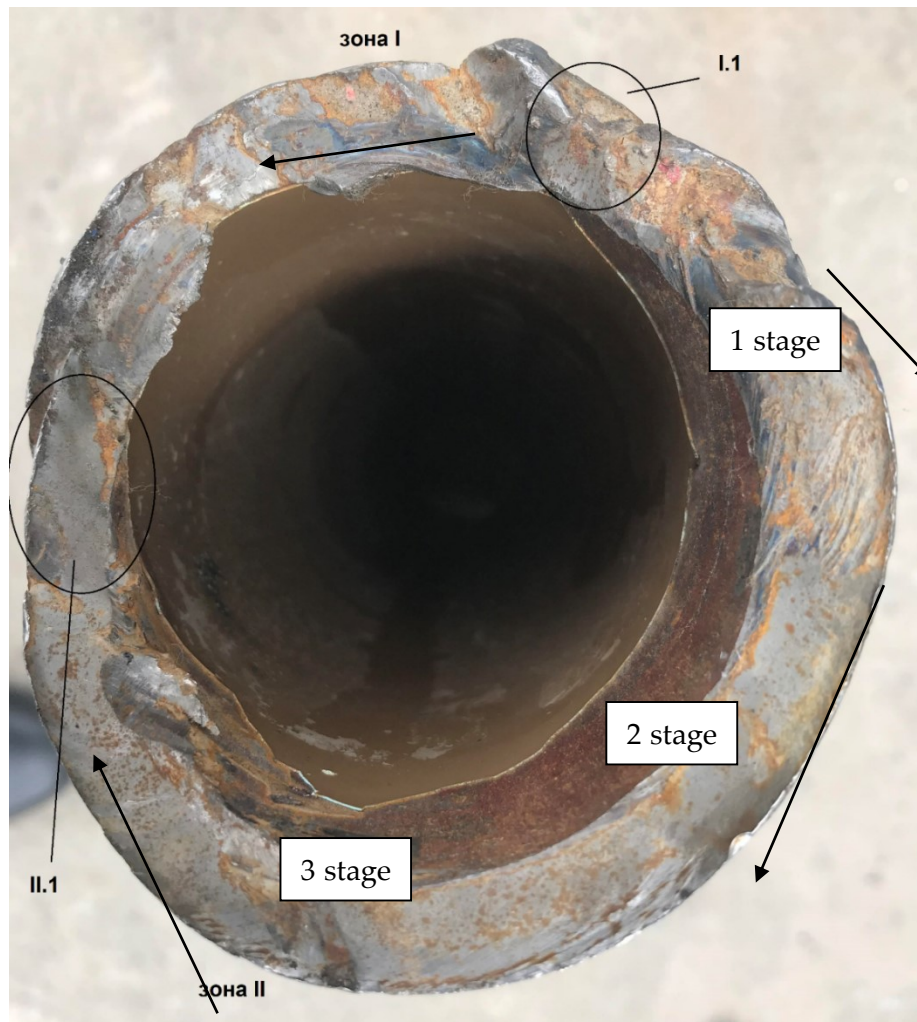


Figure 21: Broken pipe cross-section view

Drill Pipe Technical Expertise Conclusions

From section I.1, there are washouts gone in opposite directions. In clockwise direction washed out section transfer into a smoothed section of the brittle crack propagation (2nd stage in Figure 21). There are no washout traces, the shape of the pipe wall pipe is almost unchanged, tightening and chops of the cut are absent, the surface of the break is almost perpendicular to the axis of the pipe. All this indicates an accelerated propagation of the crack by a brittle mechanism under the action of stresses directed along the pipe axis, after the pressure of the drilling fluid has been released. 3rd stage of the crack propagation is characterized by a change in the angle of inclination of the fracture surface to a plane perpendicular to the axis of the pipe. This indicates the appearance of tangential stresses from torsional loads. It was not possible to bring to light more detailed features of the main crack propagation mechanism in the full fracture photo.

On the surface of the fracture (zone II) there are parallel beach marks oriented perpendicular to the crack extension, indicating the presence of cyclic loads.

Fracture surface analysis, performed by electron metallography, showed that the fracture on the F1 fragment has a honeycomb pattern that is approximately uniform over the entire surface (Figure 22). This confirms the same loading conditions during the formation of cracks in this area. Cellular relief characterizes the viscous-brittle nature of the destruction of the metal that occurs during the embrittlement of the metal with a significant margin of viscosity during the accelerated development of cracks. Thus, on the fragment of fracture F1, the crack was in the stage of accelerated development, already after reaching the critical length.

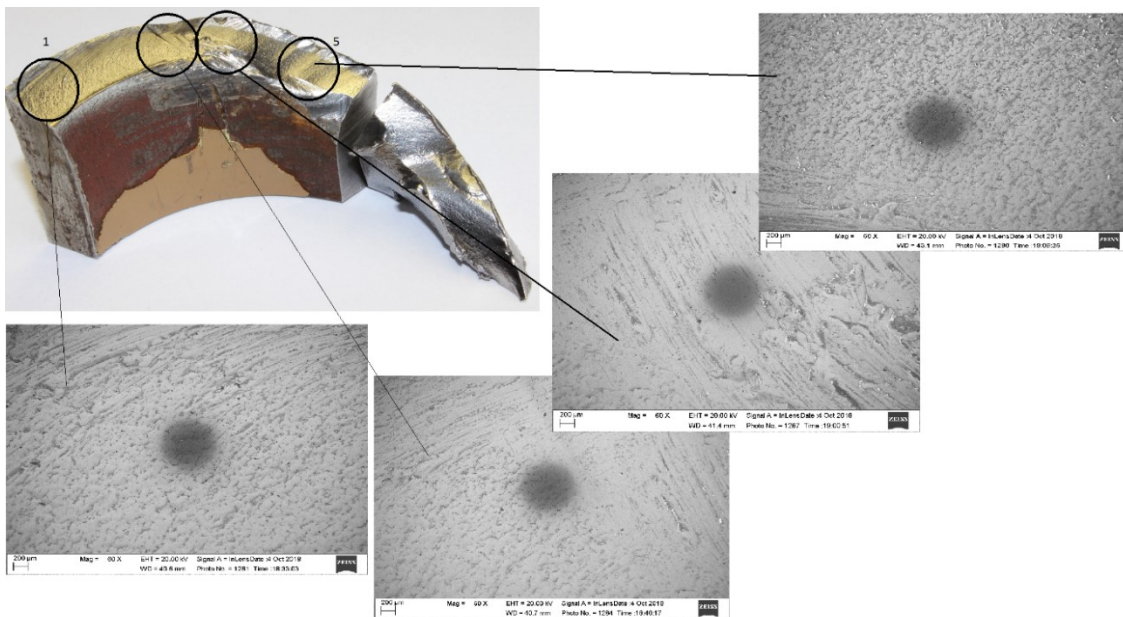


Figure 22: Fracture relief on the F1 fragment (electron metallography)

Thus, the fractography study showed that the fracture initiation proceeded in 4 stages:

Stage 1 – crack initiation on the inner surface of the pipe with an approximate length of 5-7 mm and the subsequent propagation towards the central part of the pipe wall;

Stage 2 – blind crack propagation from the center of the pipe wall to the outer surface under the wedging effect of the drilling fluid with the following pressure loss in the drill pipe;

Stage 3 – the washout zones formation along the edges of a through main crack under the pressure of drilling mud;

Stage 4 – main and secondary cracks accelerated propagation in opposite directions by brittle mechanism under the stresses from the lower BHA weight of the BHA. Rupture area occurred under the action of tangential stresses from the torque (Elagina O., Buriakin A. and Volkov A. 2018).

5.5 Number of Cycles to Failure Analysis (on samples with and without a stress concentrator)

According to the expertise, the equivalent stress value in the cross section of the drill pipe at the broken section was 176 MPa. In Chapter 4.5 of this paper, the calculated value is 377 MPa (54695 psi). This difference arises due to different initial conditions for the loading calculations. If in Chapter 4.5, the axial force is calculated from the condition that the drill string does not touch the bottomhole and is under tension, then in the expertise it is assumed that the bit rotates on-bottom with a WOB equal to 5 tons. Moreover, previously the worst-case scenario was assumed.

In any case, the endurance limit (bending with rotation) of examined drill pipes is equal to 107 – 122 MPa. The specified values are lower than the equivalent stresses acting on the broken section. Thus, the crack initiation could occur because of the fatigue accumulation from cyclic loading of the drill pipe metal.

To estimate the drill pipe metal endurance a test cycle was performed for samples cut from pieces #1 (Y1, Y2) and #2 (Y3, Y4) (Figure 23).



Figure 23: Sample marking for endurance limit test. a) Fragment #1, b) fragment #2

Drill Pipe Technical Expertise Conclusions

Two sets of samples were prepared. Each set of samples consisted of a sample without a stress concentrator (type VII according to GOST 25.502) and a sample with a modified crack-like stress concentrator (similar to type III according to GOST 25.502) simulating a germ crack formed on the surface of the pipe. Tests of specimens manufactured according to type VII should show the tendency of the metal to form cracks under cyclic loads on the fracture section and outside this area in the absence of a concentrator, and type III specimens in the presence of a concentrator. A stress concentrator on type III specimens was applied with a 0.5 mm thick mill with the formation of a linear notch 5 mm long, oriented perpendicular to the main tensile stresses.

The loads selected for cyclic tests were taken equal to $0,5\sigma_b$, which corresponds to the maximum allowable stress level in the pipe wall, and amounted (approximately 450-460 MPa). The number of loading cycles is assumed to be 200 000 cycles, which roughly corresponds to 200 days of the drill pipe operation.

Loading parameters were as follows:

- test base – 200 000 cycles;
- loading frequency – 20 Hz;
- cycle asymmetry factor – 0,5;
- cycle type - sinusoidal, of fixed sign.

The test results are presented in Table 20.

Obtained data analysis illustrates that samples Y1 and Y2, made from metal of fragment #1, showed lower resistance to cyclic loads than samples Y3 and Y4, cut from fragment #1. It means that there are no local stress concentration zones at the fracture site.

Cyclic testing of samples without a stress concentrator showed that the drill pipe metal can form cracks at stresses of 460-470 MPa per 200 000 of cycles. The presence of a stress concentrator reduces the number of cycles to failure up to 26–38 thousand cycles (Elagina O., Buriakin A. and Volkov A. 2018).

Number of Cycles to Failure Analysis (on samples with and without a stress concentrator)

| Sample marking | Sample type | Working part sizes of the sample, mm | | Stress Concentrator dimensions, mm | | Area of concentrator, mm ² | The actual cross-sectional area of the sample, mm ² | Excluding the concentrator | | With regard to the concentrator | | Number of cycles applied | Comments |
|----------------|-----------------------------|--------------------------------------|-----------|------------------------------------|-------|---------------------------------------|--|---|---|---|---|--------------------------|---|
| | | width | thickness | radius | depth | | | The minimum stress in the cycle, $1 / \sigma_b$ | Maximum stress in the cycle, $1 / \sigma_b$ | The minimum stress in the cycle, $1 / \sigma_b$ | Maximum stress in the cycle, $1 / \sigma_b$ | | |
| Y2 | Type VII * (GOST 25.502-79) | 16,60 | 3,54 | 10 | 0,63 | 2,98 | 55,78 | 0,100 | 0,500 | 0,105 | 0,527 | 26300 | Destruction with the initiation and propagation of fatigue cracks from the concentrator |
| Y4 | Type VII * (GOST 25.502-79) | 17,08 | 3,45 | 10 | 0,54 | 2,37 | 56,56 | 0,100 | 0,500 | 0,104 | 0,521 | 38244 | Destruction with the initiation and propagation of fatigue cracks from the concentrator |
| Y1 | Type III (GOST 25.502-79) | 14,57 | 3,57 | - | - | - | 52,0149 | 0,100 | 0,500 | - | - | 200 000 | The formation and propagation of fatigue cracks in the smallest section |
| Y3 | Type III (GOST 25.502-79) | 14,13 | 3,36 | - | - | - | 47,4768 | 0,100 | 0,500 | - | - | 200 000 | Without destruction |

Table 20: Cyclic loading test results

* A transverse cut made by a 0,5 mm thick diamond cutter was used as a concentrator

5.6 Structure and hardness analysis

Hardness measurements showed that the formation of a structureless layer on the fracture surfaces of the considered samples leads to a sharp increase in surface hardness to 567 HV, then the hardness decreases to the initial level at a distance of about 10 mm from the fracture surface. This indicates a significant cold-hardening of the near-surface metal layers in these areas as a result of operating loads.

The metal hardness of one of the samples in the area of the fracture going from the inner surface is much higher and exceeds the metal initial hardness by more than 80 HV. It should be noted that the increase in hardness in the crack initiation area at the outer surface on the sample is not significant, which indicates to a lower level of stresses acting during its formation. Thus, the maximum level of stress was on the inner surface of the pipe, and the outer surface was subjected to significantly less mechanical loading.

The presence of subplastic deformations that occurred on the inner surface of the pipe is confirmed by photographs made with the use of differential-interference contrast. Figure 24 shows photographs of the surface of the sample from the inner surface (a), where plastic deformation lines are visible, and from the outer surface (b), where they do not present.

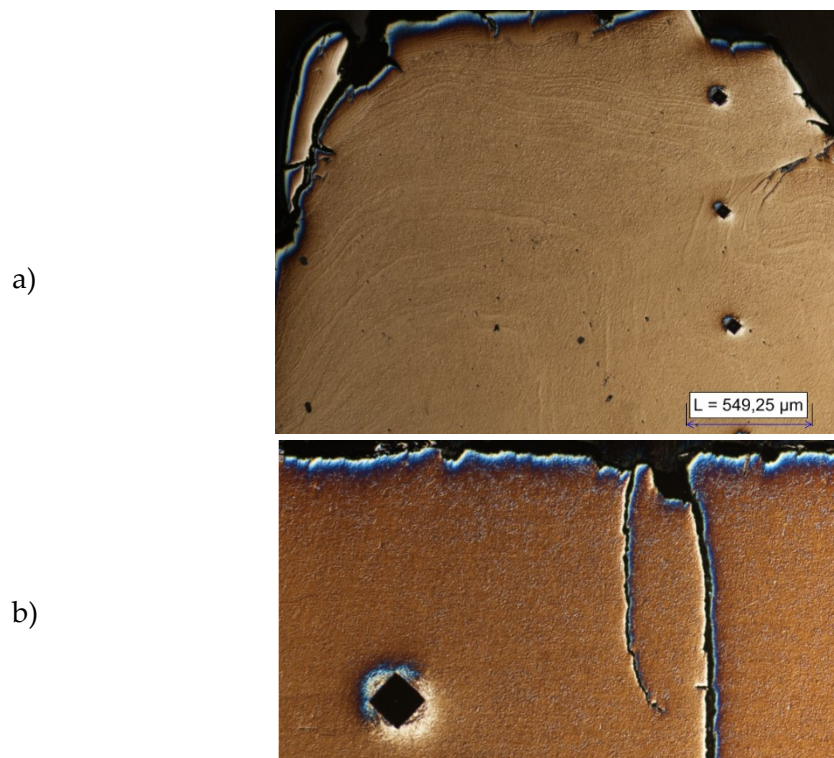


Figure 24: Sample photographs made with the use of differential-interference contrast

Drill Pipe Technical Expertise Conclusions

Thus, metallographic studies have shown that:

- The highest level of stress was on the inner surface of the pipe, where due to intense cyclic loads, fatigue cracks formed, accompanied by an increase in the metal hardness to 389 HV;
- The formation of the fracture surface during the growth of fatigue cracks was accompanied by intense work hardening, resulting in a formation of structureless amorphous layer with a hardness of up to 622 HV. Further development of cracks by the fatigue mechanism was replaced by accelerated brittle failure, not leading to a change in the structure of the surface layer;
- The outer surface of the pipe was loaded with less intensity and was destroyed by a brittle mechanism (Elagina O., Buriakin A. and Volkov A. 2018).

5.7 Mudlogging Data Analysis Based on the Technical Expertise

According to the technical expertise conclusions, the destruction occurred due to the crack initiation on the inner surface of the pipe, and its propagation under the action of cyclic loads to the central part of the wall with the subsequent development to the outer surface due to the wedging action of the drilling mud. Further development of a through-wall crack was accompanied by depressurization of the drill pipe, the formation of washout zones and subsequent opening around the pipe circumference under the action of cyclic tensile stresses with the fracture zone formation under the action of tangential stress from torque (Elagina O., Buriakin A. and Volkov A. 2018).

Therefore, it is assumed, that there is an initial washout of the drill pipe in the fracture zone with the subsequent propagation of a through-wall crack and the final loss of the tool integrity.

As a result of analyzing the mud logging data, the following observations were noted.

From 18:00 to 19:30 (06.04.18), in the Well #1, the wiper tripping was performed at a depth of 2530-2550 m. The flow rate was in the range of 17,0 – 17,3 l/s, and SPP was 163–166 bar (Figure 25).

Then, from 23:00 (04.06.18) until the tool was failed at 9:18 (05.06.18) during wiper tripping at a depth of 2550-2670 m, the flow rates were in the range of 16,9 – 17,1 l/s, and SPP was 149 – 156 bar (Figure 26).

Mudlogging Data Analysis Based on the Technical Expertise



Figure 25: Mudlogging data screenshot. Wiper trip operation from 18:00 to 19:30 (04.06.18)

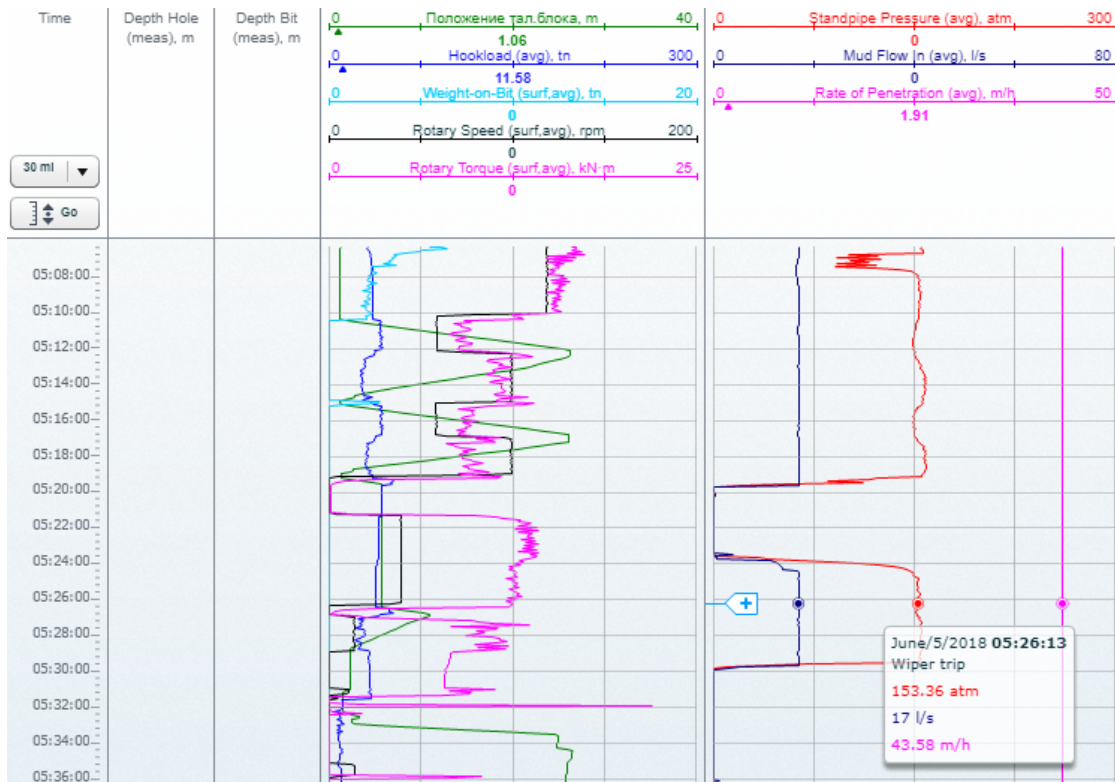


Figure 26: Mudlogging data screenshot. Wiper trip operation from 23:00 (04.06.18) to 09:18 (05.06.18)

Drill Pipe Technical Expertise Conclusions

When comparing the drilling parameters for similar operations and approximately equal flow rates, it could be noted, that there is a decrease in SPP by about 10 bar, despite an increase in the well MD.

In between of these time intervals, the sidetracking operation was performed for more than 3 hours (19:37 - 23:00, 04.06.18). It is known, sidetracking operation involves the occurrence of continuous cyclic loads in the drilling string. Probably, during this operation a through-wall washout of the drill pipe was formed, which resulted in the pressure drop described above.

Probably, a washout occurred after an increase in WOB at 22:10 (06.04.18). SPP chart shows a noticeable gradual decrease in the readings (Figure 27).

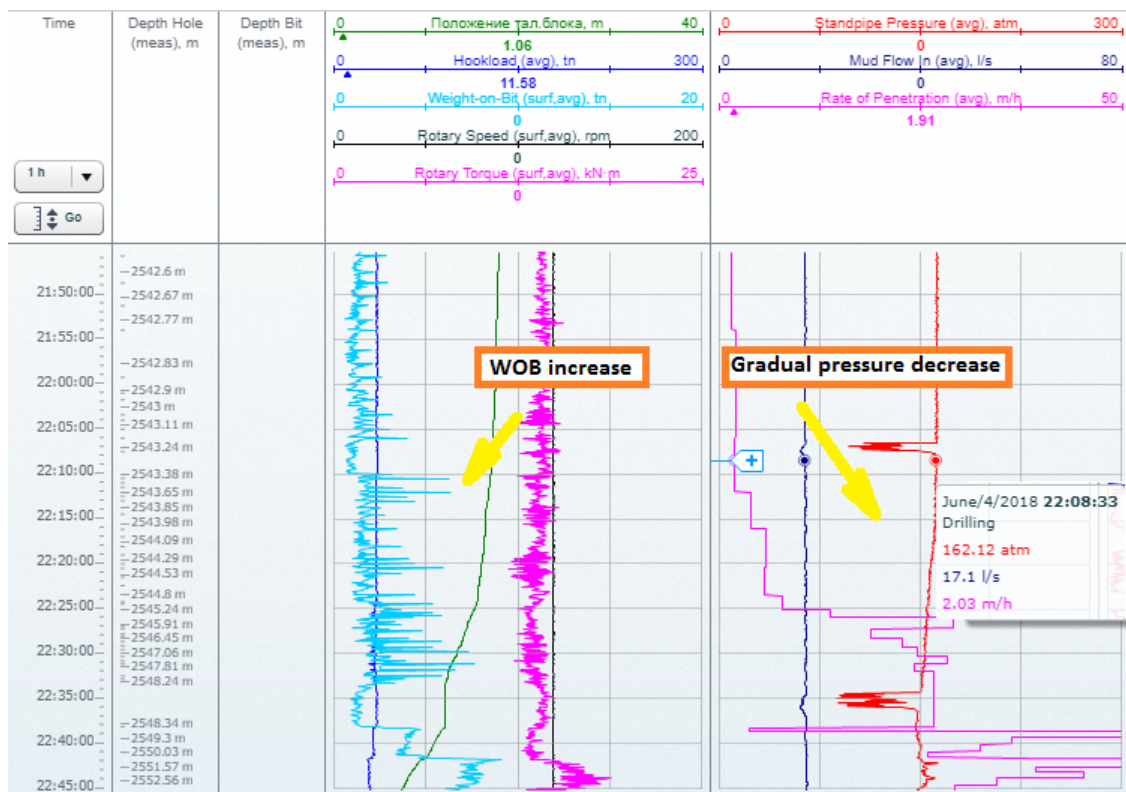


Figure 27: Gradual decrease of SPP as a probable indicator of drill string washout

Consequently, in addition to the issue of drill string condition monitoring, another significant problem arises – the problem of in-time recognition of the drill pipe washout, since most of the drill string breaks are preceded by washouts (as probably in the considered situation).

5.8 Chapter Summary

1. Analysis of the chemical composition, mechanical properties, notch toughness of the drill pipe metal showed compliance with the requirements of API 5DP and certificate №ZB17110403. It should be noted a 2-fold reduction in the actual values of the strain compared with the certificate №ZB17110403, which indicates to a significant decrease in the ductility of the metal;

2. The work of a crack initiation in the drill pipe metal is no more than 28% of the total fracture energy, which indicates the tendency of the metal to initiate cracks;
3. The values of hardness and metal structure of the drill pipe correspond to the type of heat treatment (quenching and high tempering) declared in the certificate №ZB17110403;
4. The crack propagated in 4 stages:
 - the cracks initiation from the inner surface of the pipe;
 - formation of a blind crack from the center to the outer surface under the wedging effect of the drilling fluid with a depressurization of the drill pipe;
 - formation of washout zones along the edges of a through-wall main crack under pressure of drilling mud;
 - accelerated propagation of the main and secondary cracks in opposite directions by a brittle mechanism under the action of stresses from the weight lower part of BHA with a break zone under the action of tangential stresses from the torque.
5. The calculated analysis of standard loads and impacts, that a drill pipe could have experienced in the fracture zone, showed that the total stresses in the pipe wall could exceed the fatigue strength (bending with rotation) of the G-105 drill pipes according to the Instructions (Appendix 19), however, they were significantly lower than the maximum allowed load level of $0,5\sigma_v$. Consequently, the crack initiation was caused by the accumulation of fatigue damages in the drill pipe metal as a result of cyclic loading;
6. Cyclic tests showed that the resistance to crack initiation of the drill pipe metal at maximum cycle load of $0,5\sigma_v$ is limited to approximately 200 thousand cycles in the absence of a stress concentrator and 26-30 thousand cycles in the presence of a crack-like concentrator;
7. The crack formation occurred from the inner wall of the drill pipe to the outer one, and various tests confirm the assumption that the drill pipe failure was preceded by a through-wall washout. This assumption was confirmed after analyzing the mud logging data, where a gradual SPP decrease was observed with the same operational parameters. So, there is question of a more detailed control and identification of similar signs of washouts, in order to prevent the subsequent drill pipe failures.

Chapter 6 Fatigue Analysis

6.1 Theory of Fatigue

In materials science, fatigue is the weakening of a material caused by repeated loads. It is localized structural damage that occurs when a material is subjected to cyclic loading. Fatigue is one of the most common failure sources of mechanical structures (Rabotnov 1962).

As for drilling, failure due to fatigue and lock up risks for drilling pipes in tortuous trajectory is a very costly problem in oil and gas industry. As mentioned before drill pipes and other elements receive a wide range of different kinds of loads, but the most severe for fatigue resistance are those, which affect the elements in cyclic mode.

The simplest example of that loads is a rotation of DS in axially curved region. Therefore, the element receives one stress cycle per revolution. The value of each stress cycle is determined by degree of curvature in the affected region.

Generally, axial curvature may arise due to three common reason:

- **Hole curvature:** Parts of the DS become curved as they are forced through build or drop sections of well trajectory, or around hole irregularities such as ledges, key seating etc. The accumulation of fatigue will highly influenced by the severity and location of hole curvature;
- **Buckling:** it was discussed before that buckling leads to sinusoidal or helical shaping of the DS. It happens after applying more bit weight than the string can carry remaining stable;
- **Vibration:** Vibration can cause fatigue damage by producing repeated displacements with high frequency. Fatigue due to vibrations often occurs near the bit, but may occur at other locations along the DS under different circumstances. There are several kinds of vibrations, which will be discussed later (T. H. Hill Associates, Inc 2012).

The fatigue damage accumulation leads to microcracks initiation and growth in the drill pipe body. Microcracks propagate and in combination with wall erosion come to washout. If the washed-out DS is not tripped out of hole on time, the drilling mud will initiate intensive wall erosion, which will lead to the failure accident. Previously discussed failure happened in the same order.

Microcrack fatigue formation and propagation mechanism can be more or less divided into 3 stages (Figure 28):

- In Stage 1 microscopic cracks appear on the surface of pipe body due to stress reversals in curved hole regions (A1, Figure 28);
- In Stage 2 cracks propagate perpendicularly to the applied stress into the pipe body (A2, Figure 28). The more stress level, the less time of propagation.

Moreover, crack growth rate is higher at stress concentrator areas such as upset areas, threaded tool joints places where the tongs or slips grip the pipe. Growth rates are also influenced by drilling fluid parameters. During rotation in a curved wellbore, the microcrack constantly opens and closes in cyclic stress reversal movement. When the microcrack opens, the vacuum sucks the fluid on the same principle as a pump. After the half-way of the cycle the microcrack closes and the trapped liquid inside the crack induces more severe damage due to pressure increase.

- In Stage 3 crack propagates the whole pipe wall thickness ($A_2 = S$, Figure 28), what leads to failure. The drilling mud starts to flow inside the crack under high pressure. It can wash out the pipe body within a few minutes resulting in a DS break down. Microcrack's life at stage 1 and 2 takes up to 80% of its life cycle before it can be identified by state-of-the-art defect detection methods, depending on the equipment sensitivity and metal type (Figure 29).

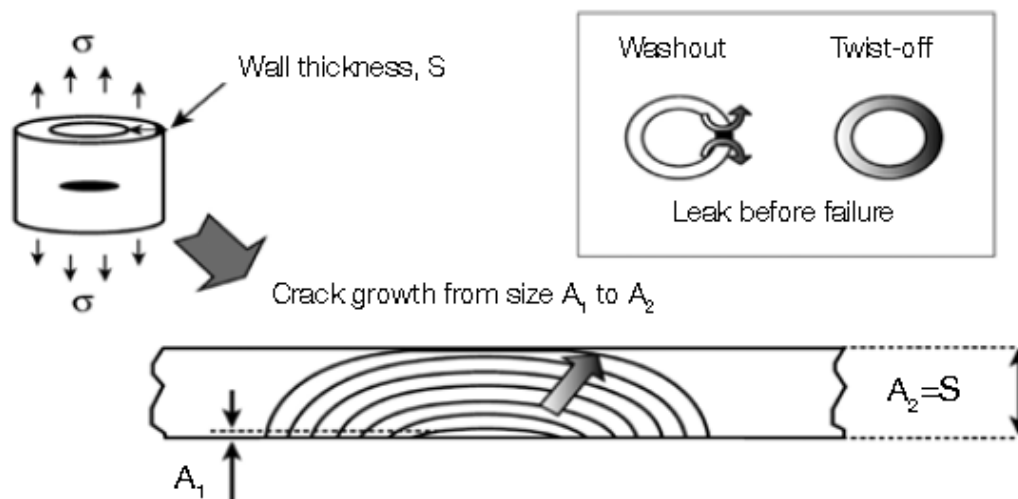


Figure 28: Microcrack development in the drill pipe body.

A_1 – initial microcrack length; A_2 – final microcrack length; S – wall thickness; σ – maximal stress direction

Since it is not easy task to detect fatigue cracks by means of non-destructive testing in early stages of crack growth, the capability to predict the cumulative fatigue wear of the DS becomes of crucial importance. The methods used today in drilling to estimate drill pipe use, such as footage, circulation hours or other cumulative physical indicators, do not provide a real data for the current condition analysis.

In order to estimate the DS condition more precisely, we need an approach, which considers as much influencing factors as we can measure and analyse (Fomin 2018).

Fatigue Analysis

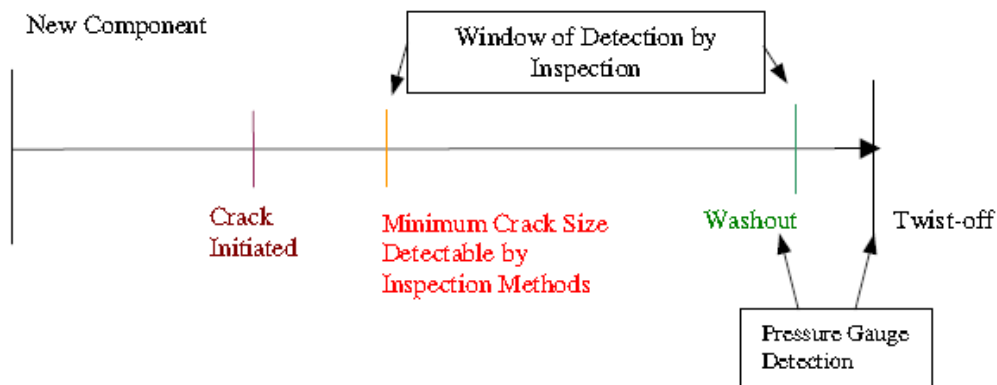


Figure 29: Crack growth propagation in the DS body (Fearnley 2003)

6.2 Implementation of TH Hill Curvature Index Approach

6.2.1 Curvature Index curves

Curvature Index is an indicator of the relative fatigue life of a drill pipe that is working in rotating mode in a curved borehole. It takes into account hole curvature, pipe weight, grade, geometry and class, and axial forces in the pipe. The derivation of these CI-curves can be found in the Vol. 2 of DS-1 Standard (T. H. Hill). An example of curve is given in Figure 30 (Hill, et al. 2005).

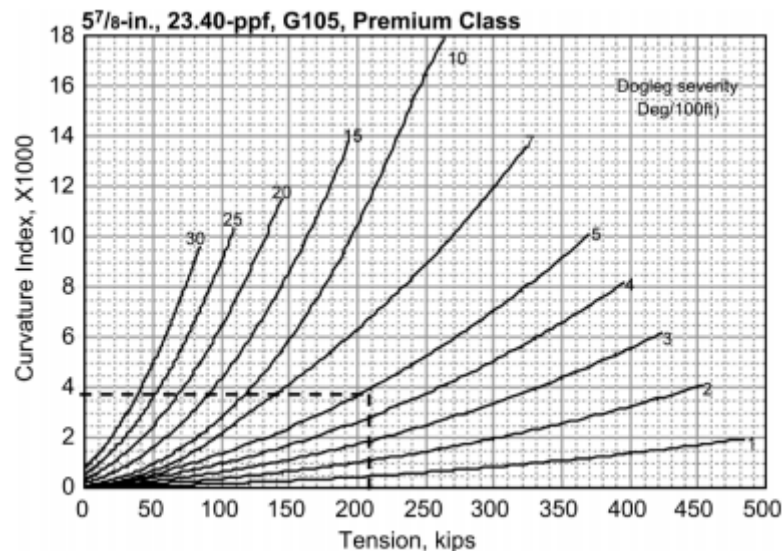


Figure 30: CI-curve for 5 7/8-in, 23.40-ppf, G-105, premium-class drill pipe

The CI is very applicatory for quantitative comparison of design alternatives. Because of big role of axial tension in the drill pipe fatigue damage, the index should be estimated for both the backreaming load case (obviously highest tension), and the rotary drilling case (active most of the time).

Let's check our pipes by maximum Curvature Index. From the actual data we know that we used 3 1/2-inch 13,3 ppf, Grade G, 1st class drill pipe in a hole section having a 6,7 degree/100 feet DLS. Torque and drag analysis show that tension while backreaming operations will be 55,000 pounds.

We consider that we work with design group 2, because drill pipes have been used before drilling horizontal section of mother well. The maximum CI for design group 2 is 10,000. Comparison of that value with real number is shown in the Figure 31.

Thus, the overloading fatigue limits for 2nd design group are not exceeded.

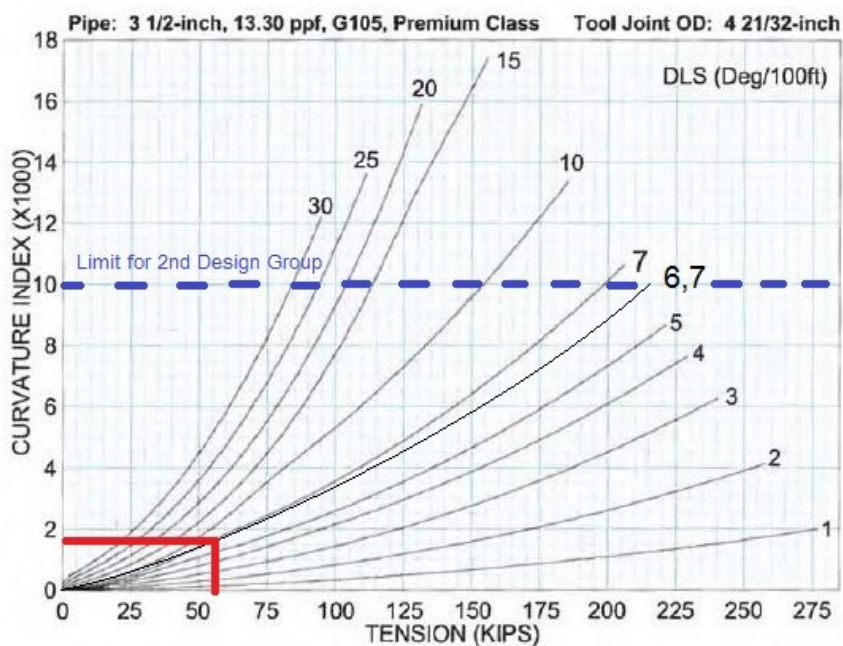


Figure 31: Comparison of the maximum CI with an applied one

6.2.2 Comparative design approach

In planning stage, engineers probably do not know size, shape, location, severity of stress concentrators, how the environment is affecting fatigue accumulation, how actual well path will look like.

Well known analytical tools, such as S-N curves, modified Goodman diagrams, etc., depend heavily on experimental data to predict fatigue behavior. The forecasts usually turn out to be just estimates. It was shown that accuracy of the forecasts is affected by the large number of parameters involved in the data received from fatigue experiments (Majumdar 1986).

Fatigue Analysis

For fatigue, most acceptable designs can still be significantly improved. The designer gains improvement by comparing available acceptable alternatives of different drill stem designs, and selecting from them the one, which suits the fatigue performance better.

In our case, we will not compare different designs; we will compare different DS intervals for accumulated fatigue. The point is to calculate "damage points" (Eq. 10) accumulated on various sections of the DS.

$$DP = \frac{\text{Cycles} \cdot CI}{10^6} = \frac{60 \cdot CI \cdot RPM \cdot Footage}{ROP \cdot 10^6} \quad \text{Eq. 10}$$

Where CI – Curvature Index;

RPM – revolutions per minute, rev/min;

Footage – the distance passed in certain operation, m;

ROP – rate of penetration, m/hour.

To obtain CI value for used drill pipes we refer to CI-curve illustrated in Figure 31.

Values for tension can be found calculated from Landmark WellPlan software. DLS is actual DLS given by directional drilling services.

Three points along the DS were chosen to compare them in a question of damage points accumulation. The Table 21 represents the distances from bit to the points of interest. Point #2 is the point of drill pipe break down.

| | Distance, m |
|----------|--------------------|
| Point #1 | 1470 |
| Point #2 | 1290 |
| Point #3 | 1120 |

Table 21: Distances for points of interest from the bit

By using mudlogging data-sheets calculations of damage points for each operation were performed. An example of such calculations is given in Figure 32.

To accumulate damage points three conditions for drill pipe are required:

1. The pipe should rotate (RPM>0);
2. The pipe should be in tension ($F_{axial}>0$);
3. The pipe should work in curved borehole interval (DLS>0).

During analysis it was found that the most of the damage points were registered while backreaming and sidetracking operations. Drilling itself does not followed by tension loads on pipes. They usually lay below the neutral point of DS being in compression state. Due to the low values of tension while RIH with rotation these operations can be neglected by our calculation.

| Time | Bit Depth, m | RPM | Point #1 depth, m | DLS, deg/100 ft | Tensile Load, kips | Curvature Index | Damage Points |
|--------------------------------------|--------------|------|-------------------|-----------------|--------------------|-----------------|---------------|
| June 5 16:00:00 | 2777,6 | 59,4 | 1307 | 4 | 20 | 1800 | 0,53442 |
| June 5 16:00:05 | 2777,4 | 59,6 | 1306 | 4 | 20 | 1800 | 0,53604 |
| June 5 16:00:10 | 2777,3 | 59,0 | 1306 | 4 | 20 | 1800 | 0,53127 |
| June 5 16:00:15 | 2777,2 | 59,3 | 1306 | 4 | 20 | 1800 | 0,53352 |
| June 5 16:00:20 | 2777,1 | 59,2 | 1306 | 4 | 20 | 1800 | 0,53235 |
| June 5 16:00:25 | 2777,0 | 59,4 | 1306 | 4 | 20 | 1800 | 0,53442 |
| June 5 16:00:30 | 2776,9 | 59,0 | 1306 | 4 | 20 | 1800 | 0,531 |
| June 5 16:00:35 | 2776,8 | 59,0 | 1306 | 4 | 20 | 1800 | 0,53127 |
| June 5 16:00:40 | 2776,6 | 59,2 | 1306 | 4 | 20 | 1800 | 0,53307 |
| June 5 16:00:45 | 2776,5 | 59,5 | 1305 | 4 | 20 | 1800 | 0,53568 |
| Total Damage Points in the interval: | | | | | | | 5,33304 |

Figure 32: Damage Points calculation example

The average damage points for each point of interest is represented in Table 22. As mentioned before in buckling analysis chosen points didn't work during the first three fishbone laterals drilling. That is why data of these fishbone branches is not in the table.

| | Side tracking/drilling | | | Backreaming | | |
|---------------|------------------------|----------|----------|-------------|----------|----------|
| | Point #1 | Point #2 | Point #3 | Point #1 | Point #2 | Point #3 |
| Main wellbore | 0 | 0 | 0 | 32 | 20 | 15 |
| FB7 | 0 | 0 | 0 | 195 | 158 | 114 |
| FB6 | 0 | 0 | 0 | 204 | 146 | 123 |
| FB5 | 0 | 242 | 43 | 236 | 302 | 209 |
| FB4 | 0 | 0 | 116 | 176 | 186 | 179 |
| Σ | 0 | 242 | 43 | 667 | 626 | 461 |

Table 22: Cumulative damage points in each branch

Finally, total cumulative damage points for investigated drill string points are the following:

- Point #1 – 843;
- Point #2 – 1054;
- Point #3 – 799.

Thus, if compare concerned drill string intervals, broken drill pipe accumulated the highest score of fatigue damage according to comparative design approach of DS-1 Standard. Estimation would be more precise and more representative if, for example,

Fatigue Analysis

each pipe stand was analyzed. Such detailed calculation requires creating an application program with estimation algorithm. Given estimation for only three points was made “by hands” in Microsoft Excel software and represents a rough estimation, but still demonstrates that the broken pipe was relatively more loaded in terms of fatigue.

6.3 Lubinski Curves

Hansford and Lubinski have developed a cumulative fatigue life evaluating method in noncorrosive and extremely corrosive environments, assuming a rotary speed of 100 RPM and drilling rate of 10 ft/hour. The results of estimation can be represented by Figure 33.

Technical expertise (Chapter 5) indicated that we deal with noncorrosive environment.

Figure 33 is for Grade E steel drill pipe only. Although fatigue experiments on small and polished specimens display great improvement with steel strength, experiments conducted on full-size joints show that fatigue characteristics either remain the same or improve very little. As a matter fact, higher strength steels displaying a greater notch sensitivity might even be inferior in fatigue performance (Lubinski and Hansford 1966).

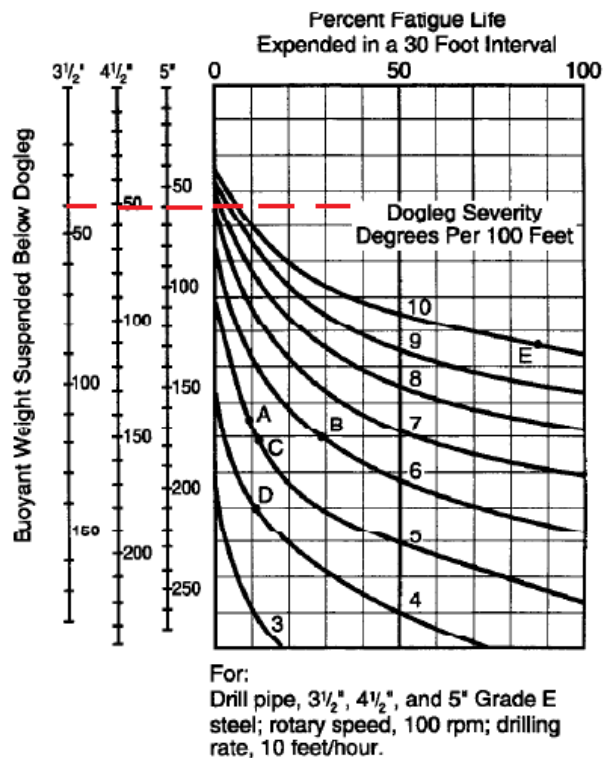


Figure 33: Fatigue damage in gradual doglegs for noncorrosive environment
(Lubinski and Hansford 1966)

The dashed line in the figure above indicates the maximum expected tension load for 3 1/2-inch broken drill pipe. Taking into account the fact that the maximum DLS along the

whole wellbore is equal to 7,6, we can conclude that there were no significant fatigue damage accumulation according to the Lubinski curves.

However, let's see one more fatigue estimation approach, which considers sharp changes in DLS along the wellbore. The schematic case of an abrupt dog-leg illustrated in Figure 34 **Ошибка! Источник ссылки не найден.** The borehole is geometrically straight (not necessarily vertical) both above and below the dog-leg. The angle by which the hole turns in the dog-leg will be referred to as "dog-leg angle". This greatest bending stress increases with the tension to which the pipe is subjected (Lubinski 1961).

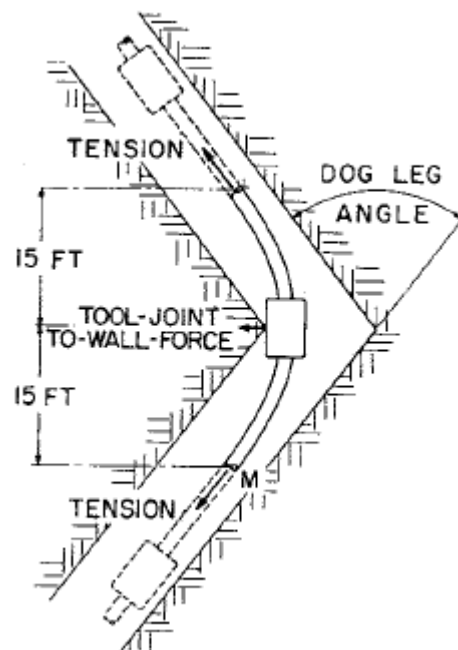


Figure 34: Abrupt dogleg

Too high values of dog-leg angle can lead to accelerated fatigue damage appearance. It is assumed only if one tool joint contacts the borehole wall (neighboring do not). The abrupt dog-leg curve for 3 1/2 -inch 13,3 lbf drill pipes is shown in Figure 35. According to the comparative design estimations range of tension in drill pipes laid between 0 and 40 kips (colored in Figure 35).

The diagram shows that in some circumstances sharp dogleg change should not exceed 2,1-3,5 DLS values. Let's analyze how abrupt were the DLS changes along the well. For that purpose actual survey data is used. The most critical MD are presented in Table 23.

As we can see in the diagram, a drill pipe which is in 20 kips tension only should not be rotated in abrupt dog-leg angle more than 3, but we defined that even in upper

Fatigue Analysis

intervals some areas have sharp DLS changes up to 4. Thus, the well trajectories are to be designed in more smooth way to avoid fatigue damage problems due to abruptness.

| MD, m | Dog-leg angle, deg/100 ft |
|--------|---------------------------|
| 480,0 | 4,0 |
| 610,0 | 2,7 |
| 740,0 | 3,8 |
| 840,0 | 4,2 |
| 870,0 | 3,3 |
| 1090,0 | 2,9 |
| 1150,0 | 3,5 |
| 1170,0 | 2,0 |

Table 23: Severe dog-leg angles along the Well #1

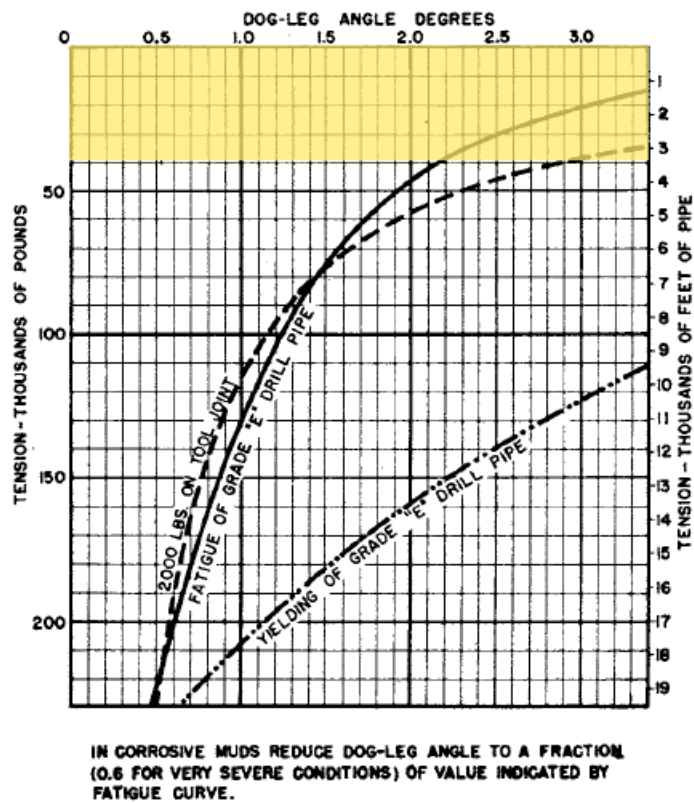


Figure 35: Abrupt dog-leg. Dog-leg angle vs tension for 3 ½ in., 13,3 lbf drill pipe

6.4 Chapter Summary

The results of fatigue analysis can be concluded as the following:

1. Considering that we deal with drill pipes of 2nd design group, the overloading fatigue limits for NWDP-88,9 x 9,35 G-105 are not exceeded;
2. If compare concerned drill string intervals, broken drill pipe accumulated the highest score of fatigue damage among three chosen points according to comparative design approach of DS-1 Standard. For more detailed analysis calculation requires creating an application program with estimation algorithm. Given estimation is only a rough calculation, but still demonstrative that the broken pipe was relatively more loaded in terms of fatigue;
3. Taking into account the DLS values and tensile loads along the whole wellbore, we can conclude that there were no significant fatigue damage accumulation according to the Lubinski curves;
4. Abrupt dog-leg angles could have destructive effect on drill pipes. Thus, well trajectories are to be designed smoother not only in horizontal sections but also in upper intervals of high tensile loads.

Chapter 7 Recommendations

7.1 Buckling effect elimination

Landmark WellPlan calculations showed that drill pipes were under the influence of sinusoidal buckling for significant amount of time. Here designers have two options:

- to limit WOB values;
- to increase the stiffness of drill string “playing” with pipe section lengths and pipe geometry.

In our case limiting WOB is quite inefficient, because, firstly, actual WOB were not too high (4-8 tn) and the further decrease would be untenable. Secondly, using RSS technology was implemented for higher ROP and fast drilling. WOB decrease would contradict with previously made technology solutions.

As for stiffness, the most common way to overcome buckling issue is to add HWDP into the drill string. Usually, if buckling occurs in tangent section (as in our case) designers should add HWDP there and be done with it (Figure 36).

It may lead to some limitations in torque and drag analysis or hydraulics, but the game is worth the candle if the optimum design would be found (Mims M. 2003).

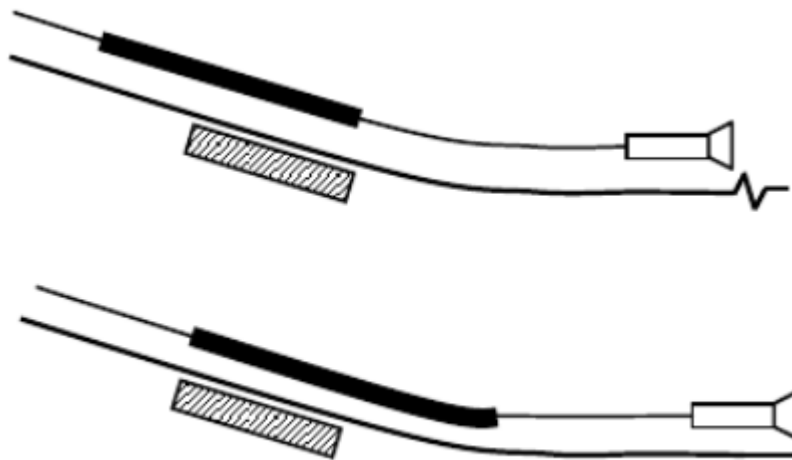


Figure 36: HWDP placing example in tangent section of drill string

Trying to implement that approach, a new drill string design was suggested by simulation in Landmark WellPlan. As a sample well Fishbone #7 was chosen.

As input value 90 kN (~9 tons) was set. It is a maximum recommended weight on a given bit. It should be noted that in previous made buckling analysis an average value for WOB_{max} was equal to 65 kN (~6,5 tons).

After some manipulations, optimal drill string design was found. The initial and transformed drill strings for the last laterals have the same sections, but different lengths (Table 10 and Table 24)

| No | Element | Length, m | Cumulative length, m | OD, mm | Element weight, tn | Cumulative weight, tn |
|----|---------------------------------------|-----------|----------------------|--------|--------------------|-----------------------|
| 1 | PDC 155,6 BT 516 US 195 | 0,2 | 0,2 | 155,60 | 0,09 | 0,09 |
| 2 | GeoPilot 5200 151 | 4,92 | 5,12 | 151,10 | 0,34 | 0,43 |
| 3 | PWD | 2,75 | 7,87 | 120,70 | 0,01 | 0,44 |
| 4 | Stabilizer | 2,00 | 9,87 | 142,90 | 0,07 | 0,50 |
| 5 | Non-magnetic Drill Collar 90x56 | 21,32 | 31,19 | 90,00 | 0,31 | 1,59 |
| 6 | Stabilizer 149,2 | 1,72 | 32,91 | 149,20 | 0,11 | 1,71 |
| 7 | Sub | 0,78 | 33,69 | 121,00 | 0,00 | 1,71 |
| 8 | HWDP-88,9 x 15,9 | 97,21 | 130,90 | 88,90 | 2,82 | 4,53 |
| 9 | NWDP-88,9 x 9,35 | 800,00 | 930,90 | 88,90 | 17,75 | 22,28 |
| 10 | HWDP-88,9 x 15,9 | 1100,00 | 2030,90 | 88,90 | 33,48 | 55,76 |
| 11 | Jar Super Bowen | 8,40 | 2039,30 | 121,00 | 0,20 | 49,22 |
| 12 | HWDP-88,9 x 15,9 | 56,18 | 2095,48 | 88,90 | 1,63 | 50,85 |
| 13 | HWDP-101,6 x 18,3 | 709,87 | 2805,29 | 102,00 | 39,86 | 90,81 |

Table 24: Suggested drill string design for Fishbone #7

Significant change was made by reduction of NWDP-88,9 x 9,35 from 1491 m to 800 m and extension of HWDP-88,9 x 15,9 from 386 m to 1100 m. Calculations gave us better results in buckling resistance. Even set value of WOB does not initiate stability losses along the string (Figure 37).

Recommendations



Figure 37: A Buckling analysis diagram for the new drill string design

To estimate the influence of such adjustment on other drilling performance parameters the following observations were made:

- ECD change is not significant and no mud window limits are exceeded;
- system pressure losses increased by 35-40%, but mud pumps still are able to withstand calculated values;
- torque and tensile load analysis satisfy existing limitations;
- the weight of DS became higher, however hook load capacity is not exceeded.

For sure, suggested DS require more investment in planning stage due to higher price of HWDP in comparison with NWDP. However, diseconomies on grounds of DS failures are incomparable with overpayment for more expensive pipe sections.

7.2 Dogleg severity control

Abrupt dog-leg angle analysis showed that in many intervals of the Well #1 too sharp dogleg changes are recorded. It is largely due to the features of designed wells, where shallow TVD go together with long horizontal tails.

Anyway in further planning and drilling the same intervals are to be excluded. Special focus should be on directional drillers work specifically while building (dropping) the angle and turn.

7.3 Drill Pipes Washouts Detection

The conclusion of Section 5.7 showed that before drill string failure broken pipe worked in washed-out condition. It means that if the washout was detected in time, the Company could avoid such large troubles.

One and only washout indicator while drilling is SPP decrease. To define 10 bars decrease by naked eye during warm work is quite impossible. That is why modern rigs are fitted with sophisticated equipment including monitoring sensors. Driller has several screens with all necessary information on them.

One of the options for driller is to set up different kinds of alarms dedicated to the drilling process. It is suggested to define recommendations for drillers of East Messoyakha field to adjust alarms for the monitoring system. Unfortunately, it is a common practice when drillers minimize the number of alarms to miss unreasonable annoying alerts.

7.4 Drill Pipes Operating Time Recording

The problem of drill stem failure analysis is still very challenging issue. It is difficult to say which loads received by single pipe during the whole life cycle. It is even impossible to record rotation and circulation time for each pipe manually not to mention loads, pressures, working intervals of tool.

Nowadays drill pipes recording is conducted by sets and we do not even know exactly did the broken pipe work in the first three fishbone of the Well #1. That is a critical point not only for failure analysis but also for failure prevention.

The current state and operations history of a single pipe can be stored only by use of technical recording means. One of the most popular trend in drilling today is the RFID (Radio Frequency Identification) technology. It is based on the radio frequency electromagnetic radiation and consists of the following components: RFID tag, RFID reader and adjusted software. The tag is to be installed into the tool joint body

The RFID technology in drilling has several disadvantages:

- sophisticated technology of installing the tag into the tool joint. It requires one more procedure in manufacturing process;
- aggregated and expensive RFID readers under the rotary table;
- decreasing of tool joint mechanical properties due to stress concentrator near the tag;
- low resistance of tags to the combined loading and wellbore environment;
- relatively high economic expenditures.

Recommendations

Due to that summary, another tagging approach is suggested in that paper – QR-coding (Quick Response Code). In comparison with RFID it does not require:

- special seats in tool joint;
- huge tag reader under the rotary table;
- internal memory to do recording.

QR-codes is a set of points to be printed on the inner side of tool joint box (the region is shown in Figure 38). This kind of print does not influence a pipe geometry and does not create new stress concentrator. There are several manufacturers of marking units, which allow putting QR-codes on the surface of drill pipe. As an example of such unit, let's take an equipment of SIC Marking Company. Marking unit parameters are listed in Table 25.

This QR-codes are not supposed to contain historical data. All data is going to be on servers and clouds.



Figure 38: Marking space for drill pipe tool joint

| SIC Marking e10D-p63 | |
|----------------------------|--------------|
| Weight, kg | 5 |
| Dimensions, mm | 261x139x211 |
| Marking Speed, symbols/sec | up to 5 |
| Marking Depth, mm | up to 0,9 |
| Metal hardness | up to 62 HRC |
| Tag reader | Yes |
| Software | Yes |
| Marking window, mm | 60x25 |
| QR-coding window, pts | 48x48 |

Table 25: SIC Marking e10D-p63 unit parameters

This QR-codes are not supposed to contain historical data. All data is going to be on servers and clouds. The depth of pipe working interval will be evaluated by bit depth data. However, the codes software and mudlogging data should be synchronized with each other to record necessary data. Procedure of drill pipe identifying and monitoring is the following:

- while RIH operation drill pipe is set to the rotary bushing;
- rig hand before lubricating the thread clean out the marking zone and reads the QR-code by device (Figure 39);
- information about new drill pipe in drill string goes to the monitoring system. Pipe started to work;
- thread lubrication and makeup connection;
- pipe (or stand) runs in hole and the history data starts to record;
- while POOH operation the same reading of tag should be fulfilled to finish history data recording.



Figure 39: QR-code reading schematics

To implement this approach a separate information system should be created. Generally, it should consist of three main parts:

1. Data base of pipes in the drilling company (drill pipe set passports);
2. Database with interface to store and process information;
3. QR-code reader software.

The database has to be incorporated with mudlogging station data, MWD data from directional drilling engineers. In perspective, it can be launched with calculation algorithms to do estimations in real-time basis.

The data base collects the following datum on drill string elements:

1. General information: type of pipe, order number, serial number;
2. Technical parameters: steel grade, thread and upset features, hardbanding, internal coating;
3. Geometry: length, pipe body diameters, tool joint diameters;
4. Current state: rate of wear, thread condition, measurement;
5. Operating time: footage, circulation hours, number of revolutions;
6. Pipe inspection and repair history: date, performed work, inspecting contractor;
7. Operation features: drilling rig, well (site), operation period;
8. Current location (O. Fomin 2019).

Recommendations

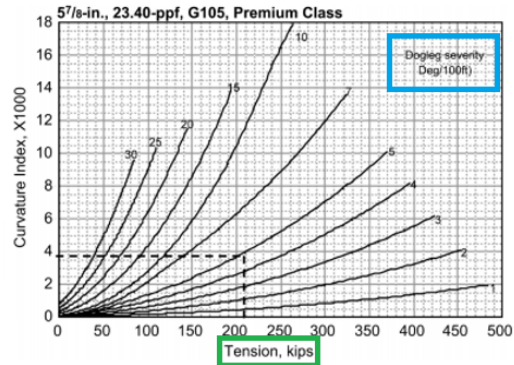
Moreover, it is possible to create a system, which will be able to estimate actual loading on drill pipes. Considering all collected data, the software would calculate tensile and bending stresses along the borehole. Buckling limits for WOB could be established too. Even fatigue life might be calculated. Because the main inputs for such calculation are time, loads, DLS and RPM.

The logic of comparative design estimation is illustrated in Figure 40.

$$DP = \frac{CI \cdot Cycles}{10^6} = \frac{CI \cdot RPM}{10^6}$$

Where CI – Curvature Index;

RPM – revolutions per minute, rev/min;



- Directional Drilling Data
- Calculated value depending on Hookload Data
- Mudlogging Data

Figure 40: Sources of data for fatigue life estimation (example of comparative design by T. H. Hill)

Thus, the idea of drill pipes monitoring and historical data recording seems to be prospective in terms of drill string breakdowns elimination due to fatigue wear and mechanical wear. It is suggested to estimate an economical efficiency of such technology realization and start to implement on the projects of PJSC Gazprom Neft.

7.5 Chapter Summary

As a result of conducted analysis the following recommendations concerning drill string integrity were described:

1. The common way to avoid buckling effects is suggested – including additional HWDP pipes into the drill string;
2. Abrupt DLS changes are to be excluded in the future. Special focus should be on directional drillers work specifically while building (dropping) the angle and turn.
3. It is suggested to define recommendations for drillers of East Messoyakha field to adjust alarms for the SPP readings in order to detect a pipe washout before the breakdown;
4. The system of each drill pipe monitoring and history recording is to be established. It might help not only in accidents analysis, but also in terms of avoiding drill string failures.

Chapter 8 Conclusions

The drill stem failure analysis is always complex procedure with wide range of possible approaches and hypothesis. The problem of failures become even more complicated when engineers encounter with accidents regularly, as it was in the East Messoyakha field. This kind of problem requires prompt initiatives implementation to avoid the same problems occurrence. Otherwise, one can not be sure that further works will be trouble-free.

The drill string failure analysis was realized in this paper by the example of Well #1 accident situation. Prior to study, drill stem regulations were reviewed in order to get acquainted with current state of drill stem elements standartization. The following key findings were obtained:

1. Static loads (such as tensile stress, equivalent stress and torque) analysis showed that no exceedance of limits were acting on drill string elements;
2. Buckling simulation in Landmark WellPlan software showed probable sinusoidal buckling initiation in the interval close to the drill pipe breakage point. Estimated operation time in buckling for broken pipe is 89 minutes, which is equivalent to 10,690 revolutions;
3. Analysis of the chemical composition, mechanical properties, notch toughness of the drill pipe metal showed compliance with the requirements of API 5DP and Quality certificate №ZB17110403;
4. The technical expertise concluded that initial crack was caused by the accumulation of fatigue damages in the drill pipe metal as a result of cyclic loading;
5. Before having the failure, through-wall washout appeared in the drill pipe body. According to the mudlogging sensors readings the well has been drilled with washed-out drill pipe for approximately 11 hours. Unfortunately, the washout could not be detected;
6. Fatigue analysis illustrated that generally there were no severe conditions for pure fatigue (combination of tension and high DLS). But still comparative design approach estimations indicated, that among three points of interest along the drill string the broken pipe received more damage points than the others. Thus, even in terms of cumulative fatigue the failed part was the most stressed;
7. Abrupt dog-leg angles were pinpointed along the wellbore trajectory, which could have destructive effect on drill pipes according to Lubinski studies.

With reference to the listed findings several recommendations were proposed concerning buckling effect elimination, DLS abrupt changes control, drill pipe washouts detection. Moreover, the system of each drill pipe monitoring and history recording suggested to establish. It might help not only in accidents analysis, but also in terms of avoiding drill string failures.

Bibliography

- Aizupe , E, and D Polyachek. *Pipes in Oil and Gas Industry. Vol. 1: Drill Pipes*. Samara: As Gard Publisher, 2012.
- Alexeev, Alexander. "Gazprom Neft: Production Line. Production Drivers and Prospective Assets." *ROGTEC*, 2017: 24-36.
- API. "5DP Standard. Specification for Drill Pipe." American Petroleum Institute, 2010.
- . "Spec 7-1 Standard. Specification for Rotary Drill Stem." American Petroleum Institute, 2006.
- . "Spec 7-2 Standard. Specification for Threading and Gauging of Rotary Shouldered Thread Connections." American Petroleum Institute, 2008.
- Clement, William P. *Writing and Thinking Well*. 2 February 2008. <http://cgiss.boisestate.edu/~billc/Writing/writing.html> (accessed July 13, 2016).
- Dongying Weima Petroleum Drilling Tools Co., Ltd. „Equipment Certificate №C-2036 for a Set of the NWDP 88,9 x 9,35 G-105, EU.“ Kogalym, 2018.
- Elagina O., Buriakin A., and Volkov A. *Drill Pipe Technical Expertise Report*. Moscow: Gublin Russian State University of Oil and Gas, 2018.
- Fearnley, Kevin. *NS-2. Drill String Inspection Standard*. Aberdeen: O.C.T.G. Procter Consultancy Limited, 2003.
- Fomin, O. "SSC: Predicting and Preventing Drill String." *ROGTEC*, 2018: 62-79.
- Fomin, O. "Identifying and Recording Drill Pipe Operating Time Using RFID Tags." *ROGTEC*, 2019: 78-92.
- Hill, T. H., & Chandler, R. B. "Field Curves for Critical Buckling Loads in Curving Wellbores." Society of Petroleum Engineers, 1998.
- Hill, T., S. Ellis, N. Reynolds, and N. Zheng. "An Innovate Design Approach to Reduce Drillstring Fatigue." *SPE Drilling & Completion*, 2005: 94-100.
- <http://www.us.bureauveritas.com/>. 2019. <http://www.us.bureauveritas.com/home/our-services/drilling-failure-prevention-and-analysis/thhill/home> (accessed February 18, 2019).
- <https://www.api.org/>. 2019. (accessed February 27, 2019).
- Kamenskikh, S. "Drilling Accidents Analysis in Timan-Pechora province." (European North Resources. Technology and Economics of Development), no. 2 (2015).
- Lubinski, A, and J Hansford. *Cumulative Fatigue Damage of Drill Pipe in Dog-Legs*. Tulsa: Society of Petroleum Engineers, 1966.
- Lubunski, A. "Maximum Permissible Dog-Legs in Rotary Boreholes." Tulsa: Society of Petroleum Engineers, 1961.

- Majumdar, Barun Kanti. "A Thesis In Mechanical Engineering." *Drill Pipe Fatigue Analysis In Offshore Application*. 1986.
- Mims M., Krepp T. *Drilling Design and Implementation for Extended Reach and Complex Wells*. Houston: K&M TECHNOLOGY GROUP, LLC, 2003.
- Mitchell, B. *Advanced Oilwell Drilling Engineering. 10th Edition, 1st Revision*. Texas: Mitchell Engineering, 1995.
- Oil and Capital Journal. "Messoyakha Field Development." <https://oilcapital.ru/>. Oil and Capital. 2017. <https://oilcapital.ru/article/tilda/20-09-2017/osvoenie-messoyahi> (accessed May 17, 2019).
- Osipov, P. *Drill String Mechanical Design*. Perm: Perm National Research Technical University, 2008.
- PJSC Gazprom Neft. «Guidance Document. Requirements for Operation and Non-destructive Testing Procedures of Drill Pipes and BHA Elements (HWDP, TWDP, Drill Collars, Subs) Gazprom Neft.» St. Petersburg , 2016.
- . <https://www.gazprom-neft.com/>. May 2015. <https://www.gazprom-neft.com/press-center/news/1108010/> (accessed May 10, 2019).
- Projects Department of Gazprom Neft. "Project Documentation. Producing Wells Construction for the PK1-3 pay zone of the East Mesoyakha field." Vol. 5.7. no. 66/14-3-IO57. Tyumen: Tyumen Scientific-Research and Development Institute of Oil and Gas, 2014.
- Rabotnov, N. *Strength of Materials*. Moscow: Fizmatgiz, 1962.
- Standard, State. «State Standard 32696-2014 Steel drill pipes for the oil and gas industry. Specification.» Moscow: Standartinform Publ., 2014.
- T. H. Hill Associates, Inc. "Standard DS-1. Drill Stem Design and Operation." Vol. 2. 2012.
- . "Standard DS-1. Drill Stem Inspection." Vol. 3. 2012.
- . "Standard DS-1. Drilling Specialty Tools." Vol. 4. 2012.
- . "Standard DS-1. Drilling Tubular Product Specification." Vol. 1. 2012.
- VNIITneft. "Drill String Mechanical Design Instruction." Moscow: VNIITneft, 1997.

Acronyms

Acronyms

| | |
|----------------|--------------------------------|
| <i>AC</i> | Alternate Current |
| <i>API</i> | American Petroleum Institute |
| <i>BHA</i> | Bottom Hole Assembly |
| <i>CI</i> | Curvature Index |
| <i>DLS</i> | Dogleg Severity |
| <i>DP</i> | Damage Points |
| <i>DS</i> | Drill String |
| <i>HD</i> | Horizontal Displacement |
| <i>HWDP</i> | Heavy-Weight Drill Pipe |
| <i>KOP</i> | Kick-Off Point |
| <i>LWD</i> | Logging While Drilling |
| <i>MD</i> | Measured Depth |
| <i>MPI</i> | Magnetic Particle Inspection |
| <i>MWD</i> | Measurements While Drilling |
| <i>NWDP</i> | Normal-Weight Drill Pipe |
| <i>PDM</i> | Positive Displacement Motors |
| <i>PJSC</i> | Public Joint Stock Company |
| <i>POOH</i> | Pull-Out-Of-Hole |
| <i>QR-Code</i> | Quick Response Code |
| <i>RFID</i> | Radio Frequency Identification |
| <i>RIH</i> | Run-In-Hole |
| <i>ROP</i> | Rate Of Penetration |
| <i>RPM</i> | Revolutions Per Minute |
| <i>RSS</i> | Rotary Steerable System |
| <i>SPP</i> | Stand Pipe Pressure |
| <i>TJ</i> | Tool Joint |
| <i>TVD</i> | True Vertical Depth |
| <i>TWDP</i> | Thick-Wall Drill Pipe |
| <i>WOB</i> | Weight On Bit |

Symbols

| | | |
|----------|-----------------------|--------------------|
| Q | force | [N] |
| k | safety factor | - |
| m | mass | [kg] |
| σ | stress | [psi] |
| A | cross-sectional area | [in ²] |
| D | diameter | [in] |
| T | tensile force | [lbs] |
| C | dogleg severity | [deg/100ft] |
| W | polar section modulus | - |
| M | torque | [N*m] |
| τ | tangential stress | [psi] |
| M | torque | [N*m] |

List of Figures

| | |
|---|----|
| Figure 1: Example of tool joint with conical shouldered connection. | 4 |
| Figure 2: Drill pipe. 1 – tool-joint box; 2 - wear-resistant coating (optional); 3 - shoulder for the elevator; 4 - weld of the coupling; 5 - planted end; 6 - pipe body; 7 - pipe body; 8 - pin weld; 9 - pin socket; 10 – tool-joint pin; 11 - rotary shouldered connection. | 6 |
| Figure 3: A Gazprom Neft production cluster in the north of the Yamalo-Nenets Autonomous Region (PJSC Gazprom Neft 2015)..... | 13 |
| Figure 4: Well profile..... | 17 |
| Figure 5: 3-D well profile | 18 |
| Figure 6: Schematics of washout and breakdown accidents on one of the well pads | 23 |
| Figure 7: 3-D profile of the Well #1..... | 25 |
| Figure 8: Mudlogging sensors readings at the moment of accident | 26 |
| Figure 9: BHA schematics left in the Well #1 | 27 |
| Figure 10: Limiting tensile loads along the drill stem in Well #1 while main wellbore drilling.. | 30 |
| Figure 11: Tensile load distribution during different operations..... | 31 |
| Figure 12: The photo of broken drill pipe (NWDP 88,9 x 9,35 G-105)..... | 32 |
| Figure 13: The torque distribution along the string in the main hole of Well #1 | 33 |
| Figure 14: Buckling schematics: a) Sinusoidal, b) Helical. | 35 |
| Figure 15: Sections where buckling is most likely to occur..... | 37 |
| Figure 16: Example of the mudlogging data-sheet buckling analysis | 40 |
| Figure 17: Tri-axial stress state transition into the equivalent stress | 43 |
| Figure 18: Two pieces of broken pipe delivered for the expertise | 47 |
| Figure 19: Longitudinal cross-section of the pipe..... | 50 |
| Figure 20: Lateral cross-section of the pipe | 50 |
| Figure 21: Broken pipe cross-section view | 51 |
| Figure 22: Fracture relief on the F1 fragment (electron metallography) | 52 |
| Figure 23: Sample marking for endurance limit test. a) Fragment #1, b) fragment #2 | 53 |
| Figure 24: Sample photographs made with the use of differential-interference contrast..... | 56 |
| Figure 25: Mudlogging data screenshot. Wiper trip operation from 18:00 to 19:30 (04.06.18) | 58 |
| Figure 26: Mudlogging data screenshot. Wiper trip operation from 23:00 (04.06.18) to 09:18..... | 58 |
| Figure 27: Gradual decrease of SPP as a probable indicator of drill string washout | 59 |
| Figure 28: Microcrack development in the drill pipe body..... | 62 |
| Figure 29: Crack growth propagation in the DS body (Fearnley 2003)..... | 63 |
| Figure 30: CI-curve for 5 7/8-in, 23.40-ppf, G-105, premium-class drill pipe..... | 63 |
| Figure 31: Comparison of the maximum CI with an applied one..... | 64 |
| Figure 32: Damage Points calculation example | 66 |
| Figure 33: Fatigue damage in gradual doglegs for noncorrosive environment (Lubinski and Hansford 1966)..... | 67 |
| Figure 34: Abrupt dogleg..... | 68 |
| Figure 35: Abrupt dog-leg. Dog-leg angle vs tension for 3 ½ in., 13,3 lbf drill pipe..... | 69 |
| Figure 36: HWDP placing example in tangent section of drill string..... | 71 |
| Figure 37: A Buckling analysis diagram for the new drill string design..... | 73 |
| Figure 38: Marking space for drill pipe tool joint | 75 |
| Figure 39: QR-code reading schematics..... | 76 |
| Figure 40: Sources of data for fatigue life estimation (example of comparative design by T. H. Hill)..... | 77 |

List of Tables

| | |
|---|----|
| Table 1: Drilling Tubular Products Covered by API and DS-1 Manufacturing Specifications | 8 |
| Table 2: Inspection Methods Covered by this Guidance Document | 12 |
| Table 3: The stratigraphic well profile with the cavernosity ratio..... | 14 |
| Table 4: The lithological well profile | 15 |
| Table 5: Mother borehole profile..... | 17 |
| Table 6: Branch borehole profile | 17 |
| Table 7: Used drill pipes and recommended drilling parameters..... | 19 |
| Table 8: Summary of washout and breakdown accidents on one of the well pads | 22 |
| Table 9: NWDP-88,9 x 9,35 G-105 characteristics..... | 28 |
| Table 10: Drill stem used in Well #1 | 29 |
| Table 11: Maximal tensile loads received by drill stem in all branches of the Well #1 | 31 |
| Table 12: Maximal torque values received by drill stem in all branches of the Well #1..... | 34 |
| Table 13: Input data for buckling analysis..... | 38 |
| Table 14: Summary of WOB _{max} for all Well #1 branches..... | 39 |
| Table 15: Buckling time for Main borehole of Well #1 | 41 |
| Table 16: Buckling time summary for Well #1 laterals..... | 42 |
| Table 17: Input and output data of tri-axial stress analysis..... | 45 |
| Table 18: Comparison of chemical analysis data | 49 |
| Table 19: Comparison of mechanical properties..... | 49 |
| Table 20: Cyclic loading test results..... | 55 |
| Table 21: Distances for points of interest from the bit..... | 65 |
| Table 22: Cumulative damage points in each branch | 66 |
| Table 23: Severe dog-leg angles along the Well #1 | 69 |
| Table 24: Suggested drill string design for Fishbone #7 | 72 |
| Table 25: SIC Marking e10D-p63 unit parameters..... | 75 |